Report HSRI-71-129

TIRE TRACTION GRADING PROCEDURES AS DERIVED FROM THE MANEUVERING CHARACTERISTICS OF A TIRE-VEHICLE SYSTEM

VOLUME II

P. Fancher
L. Segel
C. MacAdam
H. Pacejka

Final Report
Contract No.: 1-35715

Prepared for:

Tire Systems Section
Office of Vehicle Systems Research
National Bureau of Standards
Washington, D.C.

June 13, 1972

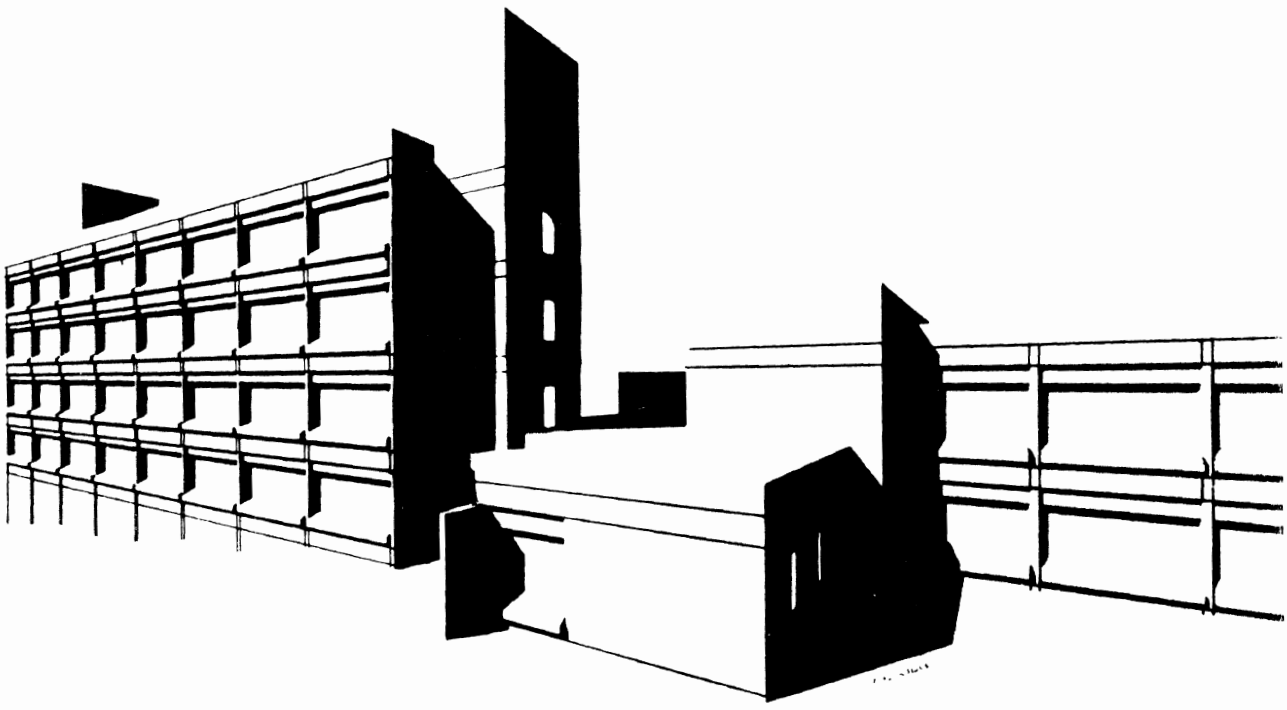

HIGHWAY SAFETY RESEARCH INSTITUTE
THE UNIVERSITY OF MICHIGAN ANN ARBOR

Report HSRI-71-129

TIRE TRACTION GRADING PROCEDURES AS DERIVED FROM THE MANEUVERING CHARACTERISTICS OF A TIRE-VEHICLE SYSTEM

VOLUME II

P. Fancher
L. Segel
C. MacAdam
H. Pacejka

Highway Safety Research Institute
Institute of Science and Technology
The University of Michigan
Ann Arbor, Michigan 48105

June 13, 1972

Final Report
Contract No.: 1-35715

Prepared for:
Tire Systems Section
Office of Vehicle Systems Research
National Bureau of Standards
Washington, D.C.

This report was prepared in fulfillment of the National Bureau of Standards Contract No. 1-35715 (funded by the National Highway Traffic Safety Administration through the NBS, Contract FH-11-6090). The opinions, findings, and conclusions expressed in this publication are those of the authors and not necessarily those of the National Bureau of Standards nor the National Highway Traffic Safety Administration.

PREFACE TO VOLUME II

The work reported in this volume was completed under contract number 1-35715. However, the results reported in either Volume I or Volume II can be understood without the other volume. The tire shear-force representation methods, which are described herein, were not used to obtain the findings presented in the first volume.

The purpose of this volume is to provide a comprehensive description of tire shear force performance for use in highly advanced simulations of combined steering and braking passenger-car maneuvers. Two approaches are presented: first, an extended tire model; and second, a mathematical method (called "the similarity method") for fitting tire data.

This work was carried out primarily by Hans Pacejka.

ACKNOWLEDGEMENTS

Mr. Philip Grote programmed the brush-type tire model. Mr. Thomas Post carried out the calculations for the similarity method example. Ms. Jeannette Nafe typed the extensive sets of equations included in this report. The authors thank these people for their contributions.

TABLE OF CONTENTS

SECTION 1

ANALYTIC SOLUTION FOR BRUSH-TYPE TIRE MODEL

The model employed consists of one or more rows of elastic studs (tread elements) which are inbedded in the rigid rotating wheel. Over a certain length, 2a, these elements make contact to the road surface. For simplicity, uniform pressure distribution, q_z, and constant elastic properties, $k_{x,y}$, are assumed throughout the contact area. The coefficient of friction, μ, is represented by a linearly decaying function of the sliding speed, V_s.

When the response to purely lateral or longitudinal slip is studied, or when equal lateral and longitudinal slip stiffnesses are considered, the tread elements deflect in the same direction as the direction of the shear force acting at the tip of the elements in the sliding range. Consequently, they deflect opposite to the direction of sliding speed of the elements with respect to the ground. In these simple cases all the elements throughout the contact range deflect in the same direction. It is assumed that the elements instantaneously assume the new equilibrium position as soon as the sliding range is entered. Due to the uniform pressure distribution the deflection remains constant in the sliding range. Also, due to the uniform pressure distribution and the simple construction of the model (carcass deflection zero or uniform) the sliding speed is known for each element in the sliding range and is equal to the slip speed, V_c, of the lower portion of the wheel. Figure 1 illustrates the situation under combined lateral and brake slip for equal longitudinal and lateral stiffnesses of the elements.

a)

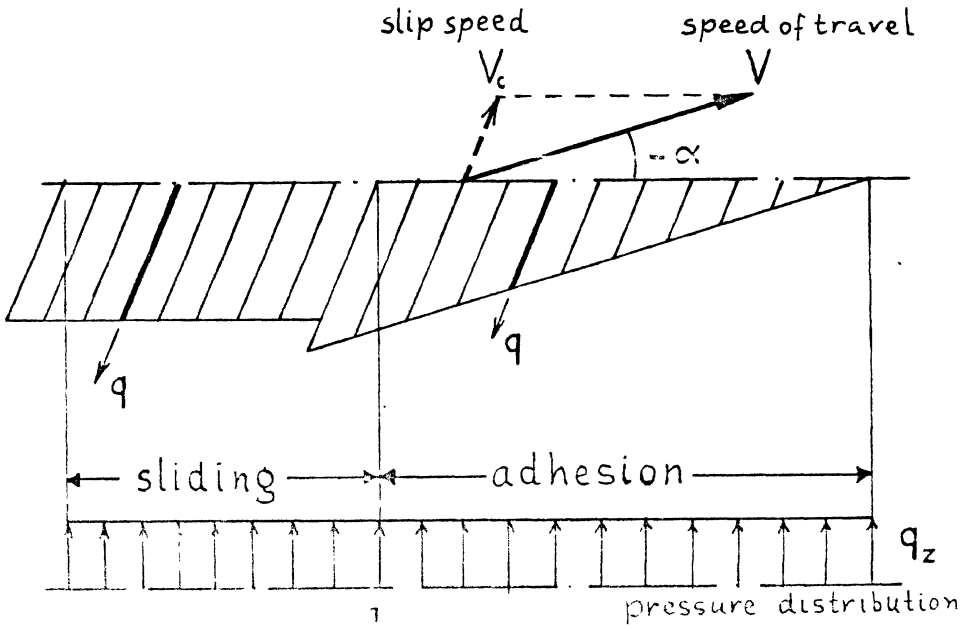

b)

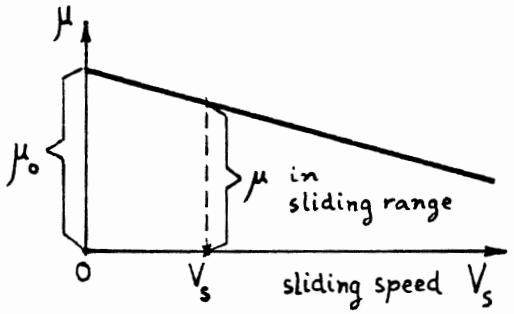

Figure 1. a) The brush type tire model under combined longitudinal (brake) slip and lateral slip in case of equal longitudinal and lateral stiffnesses.

b) The linearly decaying friction coefficient.

In case of unequal stiffnesses the deflections of the elements remain equally directed along the contact line as long as the elements remain adhered to the ground. In this adhesion range, the shear forces have not the same direction as the deflections and consequently deviate from the direction of the slip speed, V_c. In the sliding region, however, the shear force will be directed opposite to the sliding speed which, when equilibrium has been reached, equals the slip speed of the wheel, V_c. A picture as shown in Figure 2 is expected to occur.

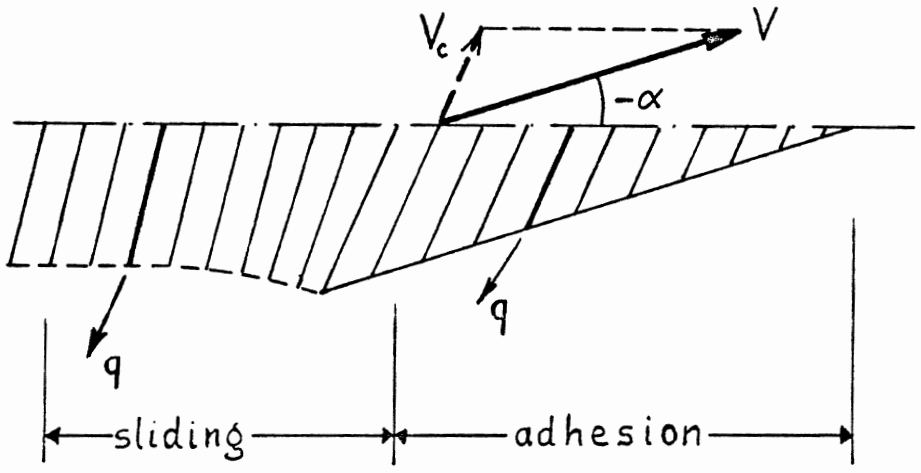

Figure 2. Expected deflection in case of unequal stiffnesses.

An exact description of the variation of the deflection in the sliding area is difficult to obtain. We will present here an approximate expression for the side force and the longitudinal force by assuming an approximate variation of the deflection of the tread element in the sliding region. We might assume that at entering the sliding zone an instantaneous drop of the deflection to the equilibrium or steady state deflection takes place. This may occur approximately when sufficient damping is provided in the rubber elements so that slip-stick is just suppressed. In the cases of purely side-slip or purely longitudinal-slip or when the slip stiffnesses are equal, no difficulty arises when adopting this assumption. In the case of unequal stiffnesses and combined inputs, this assumption may lead to an unrealistic transition from just adhesion to sliding. Consider Figure 3 which shows the situation at the transition point when instantaneous transition to the steady state deflection is assumed and the element stiffnesses in y- and x- directions (k_x, k_y) are unequal. The radii of the circle and ellipse constitute the directions of force and deflection respectively.

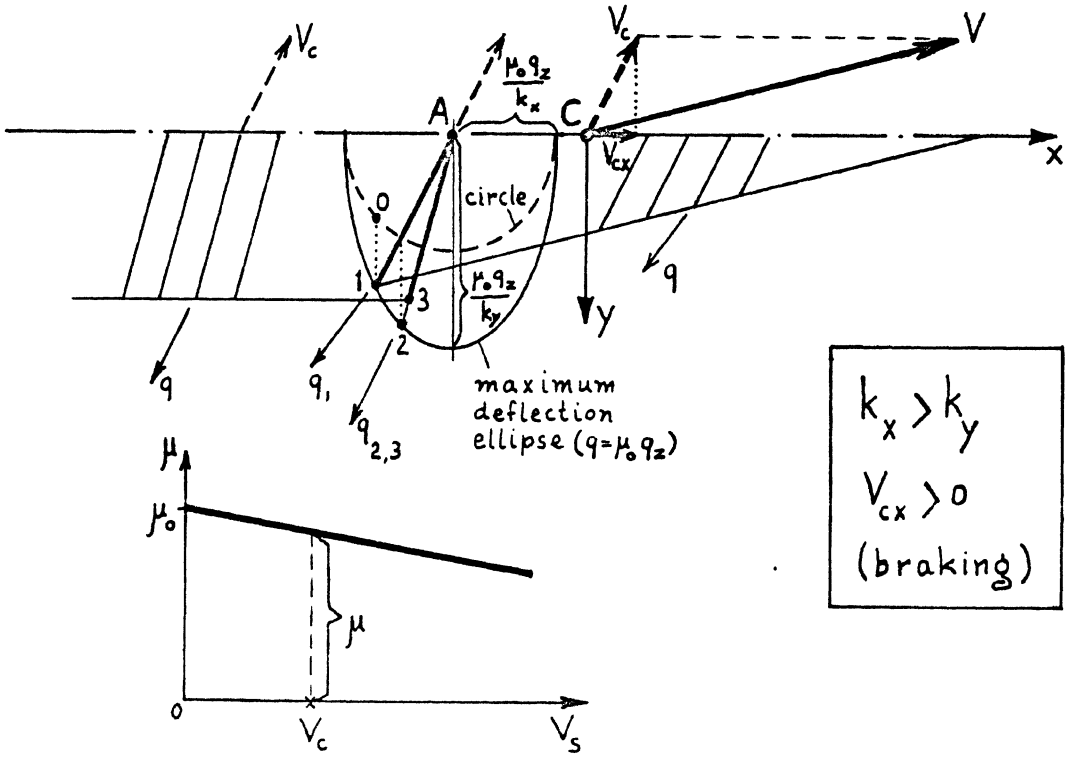

Figure 3. The instantaneous transition from adhesion to equilibrium (steady state) deflection (1→3).

At point 1 the adhesion boundary is reached ($\mu=\mu_o$). In case μ would be a constant and equal to μ_o, the tip of the element must follow the ellipse for the shear force to remain the same. In point 2 we have a shear force direction opposite to the slip speed, V_c, which is the same as the sliding speed of the element, V_s, in case equilibrium has been reached and no further change in deflection occurs. In point 3 the shear force is reduced to a value which corresponds to the lower coefficient of friction μ at $V_s=V_c$.

The figure shows that the tip has moved from point 1 to point 3 in a direction which is far from compatible with the direction of the shear force (q_1) (= direction AO).

In reality (assuming μ constant and equal in all directions), the sliding speed is directed opposite to the shear force and initially will be directed according to $\overline{OA}$. Subsequently, the sliding speed will tend asymptotically to the steady state direction ($\overline{1A}$) equal to the direction of the slip speed, V_c (cf. Figure 4).

As an approximation of the actual path of the tip of the element we take first a straight line in the initial sliding direction and second the asymptote shown in Figure 4. In the first part, which will be called the transition region, the deflection will be assumed to vary linearly from the deflection in the transition point, where sliding starts, to the steady state deflection in the point where the asymptote is reached and, presumedly, the steady state deflection commences. Figure 5 illustrates the approximate variation of the deflection.

Although in reality the picture becomes much more complicated in the case where μ depends upon the sliding speed, we will assume a similar approximate variation for the deflection. The adhesion, transition, and steady state regions along the contact length of the tire model may be found as follows.

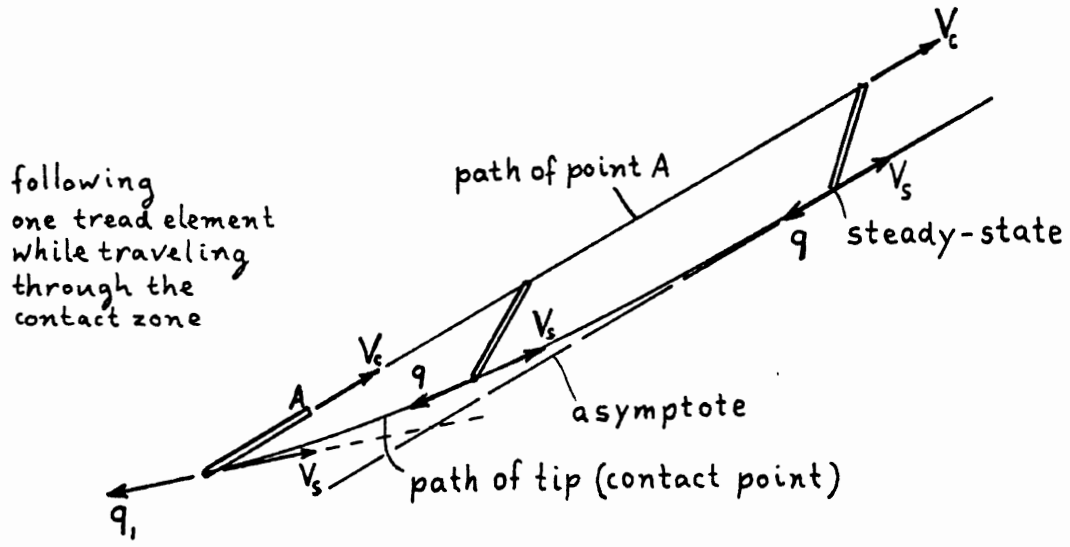

Figure 4. The variation of the deflection of a tread element with unequal horizontal stiffnesses after that sliding has started.

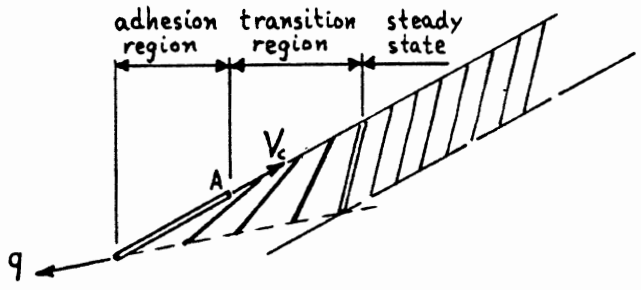

Figure 5. Approximation of variation of Figure 4.

First we derive the components of the deflection in the x- and y- directions in the transition point (u_a, v_a) and in the steady state range (u_s, v_s) as indicated in Figure 6. They correspond to point 1 and point 3 of Figure 3 respectively.

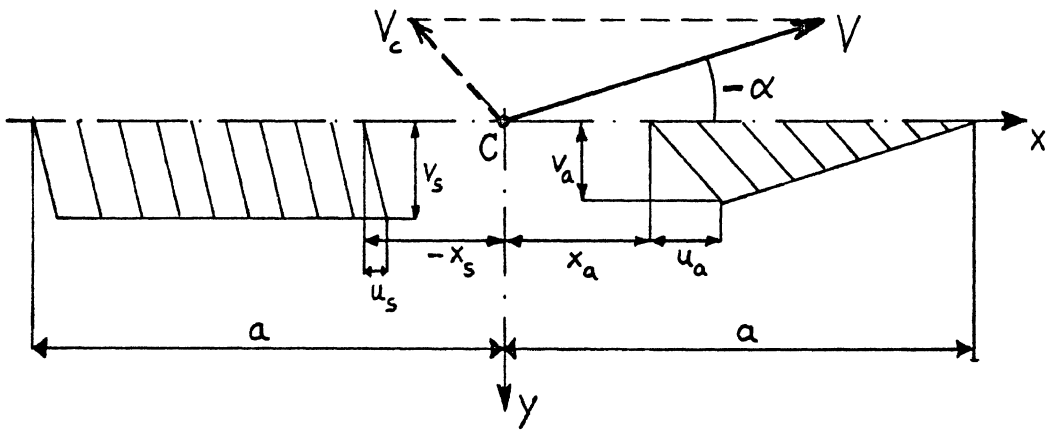

Figure 6. The deflections (u_a, v_a) and (u_s, v_s) at beginning and end of the transition region.

We define the components of the speed of travel and the slip speed :

$$V_x = V \cos \alpha, \qquad V_y = V \sin \alpha \tag{1}$$

$$V_{cx} = s_x V_x, \qquad V_{cy} = V_y = s_y V_x \tag{2}$$

with

$$s_x = V_{cx}/V_x, \qquad s_y = V_{cy}/V_x = \tan \alpha \tag{3}$$

where s_x and s_y are the longitudinal and lateral slips, respectively. As usual, the slip angle is denoted by α. The speed of rolling is defined as

$$V_r = V_x - V_{cx} = (1 - s_x)V_x \tag{4}$$

The deflections in the adhesion region become (a = half contact length):

$$\left.\begin{aligned} u &= -(V_{cx}/V_r)(a-x) = -s_x(a-x)/(1-s_x) = -s'_x\,(a-x) \\ v &= -(V_{cy}/V_r)(a-x) = -s_y(a-x)/(1-s_x) = -s'_y\,(a-x) \end{aligned}\right\} \tag{5}$$

in which have been introduced the reduced slips:

$$s'_x = V_{cx}/V_r, \qquad s'_y = V_{cy}/V_r \tag{6}$$

The shear forces per unit length of circumference, q_x and q_y, become with k_x and k_y representing the stiffnesses per unit length of the tread elements in the x- and y- directions, respectively:

$$q_x = k_x u, \qquad q_y = k_y v \tag{7}$$

At the boundary of adhesion where $x=x_a$ the resultant shear force obtains its maximum value $\mu_o q_z$. We find for x_a:

$$x_a = a - \mu_o q_z \, V_r/(k_x^2 V_{cx}^2 + k_y^2 V_{cy}^2)^{1/2}$$

$$= a - \mu_o q_z/(k_x^2 s_x'^2 + k_y^2 s_y'^2)^{1/2} \tag{8}$$

With (5) and (6) we find the deflection at the transition point:

$$u_a = -(V_{cx}/V_r)(a-x_a), \qquad v_a = -(V_{cy}/V_r)(a-x_a) \tag{9}$$

$$= -s'_x(a-x_a), \qquad = -s'_y(a-x_a)$$

As to finding the steady state deflection we must consider the fact that the sliding speed, V_s, is equal to V_c. Now V_s is known, μ can be obtained from a given functional relationship with V_s. For instance:

$$\mu = \mu_o(1-A_s V_s) \tag{10}$$

The resultant shear force equals:

$$q = \mu q_z \tag{11}$$

and is directed opposite to V_c so that

$$q_x = -(V_{cx}/V_c)\mu q_z, \qquad q_y = -(V_{cy}/V_c)\mu q_z \tag{12}$$

and further the deflections:

$$u_s = -\frac{V_{cx}\mu q_z}{V_c \, k_x}, \qquad v_s = -\frac{V_{cy}\mu q_z}{V_c \, k_y} \tag{13}$$

With the quantities (9) and (13) we are able to establish the transition length, t.

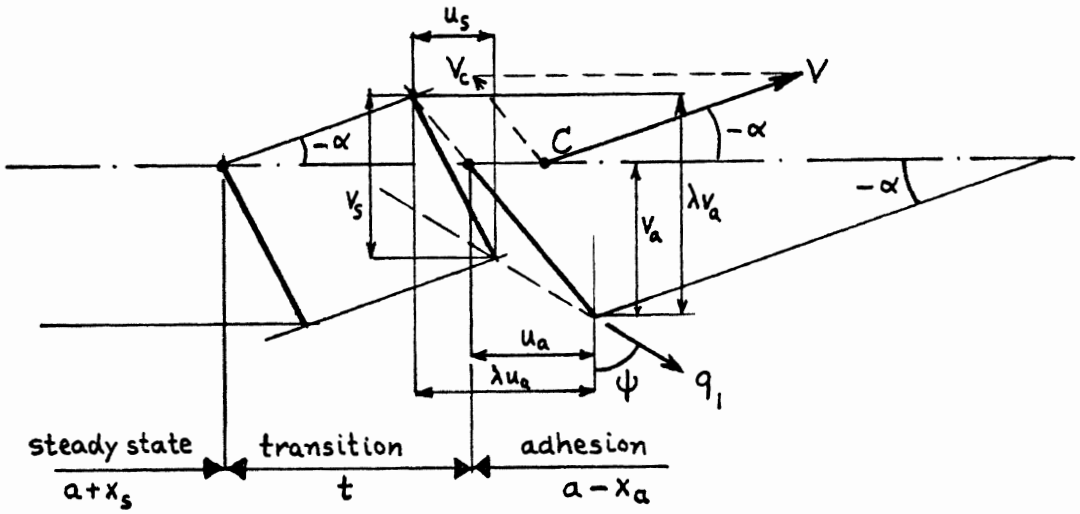

Figure 7. Graphical construction of the transition length.

The angle ψ indicating the direction of initial sliding (cf. Figure 7) is given by the direction of the internal stress

$$\tan \psi = u_a k_x / v_a k_y \tag{14}$$

With the introduction of a factor λ we have, according to Figure 7:

$$(\lambda u_a - u_s)/(\lambda v_a - v_s) = \tan \psi \tag{15}$$

With the aid of the expressions for the deflection (9) and (13) and for x_a (8) we obtain

$$\lambda = \frac{\mu(k_x+k_y)}{\mu_o k_x k_y V_c} \sqrt{k_x^2 V_{cx}^2 + k_y^2 V_{cy}^2} \tag{16}$$

For the transition length, t, we have according to the above figure:

$$t = (\lambda-1)(-v_a \operatorname{cotan} \alpha + u_a) = (\lambda-1)(a-x_a) \tag{17}$$

which results in:

$$t = (\lambda-1)\, \mu_o q_z\, V_r (k_x^2 V_{cx}^2 + k_y^2 V_{cy}^2)^{-1/2} \tag{18}$$

It may be noted that t increases with decreasing values of V_{cx} and V_{cy} as a ratio to the rolling speed, V_r. At wheel lock we have $V_r=0$ and, consequently, a vanishing transition region. In the latter case the steady state deflection occurs over the whole contact length. The resulting shear force then opposes the direction of the speed $V=V_c=V_s$. The x-coordinate where the steady state sliding region begins reads:

$$x_s = x_a - t \tag{19}$$

which with (8), (16), and (17) appears to become

$$x_s = a - \mu q_z \frac{k_x + k_y}{k_x k_y} \frac{V_r}{V_c} \tag{20}$$

Let us consider the variation of the various regions with increasing slip speed, V_c (cf. Figure 8). Below a critical value of slip, which results from equation (8) for $x_a = -a$, complete adhesion will occur in the entire contact range $-a<x<a$. When the slip is increased beyond this critical value, a sliding region will arise at the trailing edge. The transition region may extend beyond the contact length. Only the portion inside the contact range is of importance. When the sliding region becomes sufficiently large the steady state region may emerge.

For the tire model with uniform pressure distribution the adhesion region and with the transition region will vanish only in case of wheel-lock ($V_r=0$). This obviously also occurs when $\alpha=90°$. The steady state deflection extends then over the whole contact length.

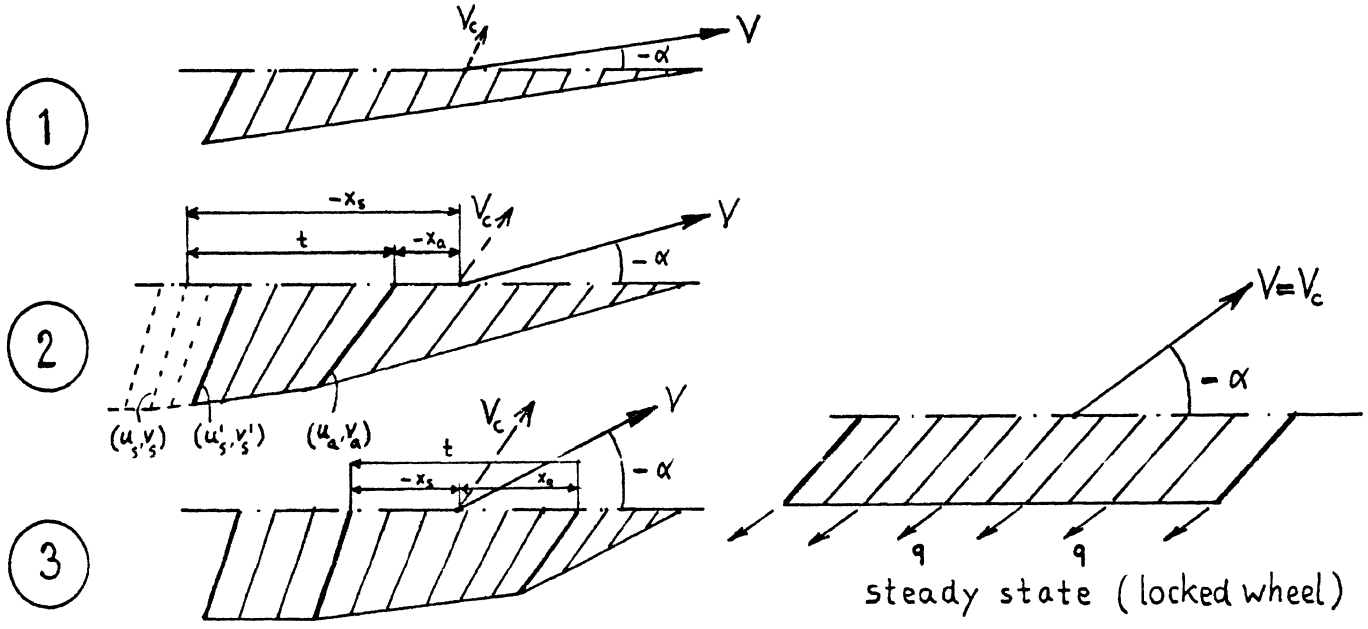

Figure 8. The various regions in the contact area at increasing values of slip.

For the computation of the resulting shear forces and the aligning moment it is necessary to consider three ranges:

Range 1 : $x_a \leq -a$ (complete adhesion)

Range 2: $x_a > -a$ and $x_s < -a$ (adhesion and transition regions)

Range 3: $x_s \geq -a$ (adhesion, transition and steady-state regions)

For a rectangular contact area with length 2a we have the following general expressions for the forces:

$$F_x = 2b \int_{-a}^{a} q_x dx, \qquad F_y = 2b \int_{-a}^{a} q_y dx \tag{21}$$

We may consider a pure translation of the base line of the tread elements due to tire carcass longitudinal and lateral flexibility. With carcass stiffnesses K_x and K_y we obtain for the resulting moment about the vertical axis through the wheel center (cf. Figure 9):

$$M_z = M'_z + F_x F_y (1/K_x - 1/K_y) \tag{22}$$

where

$$M'_z = \int_{-a}^{a} \{q_y(x+u) - q_x v\}\, dx \tag{23}$$

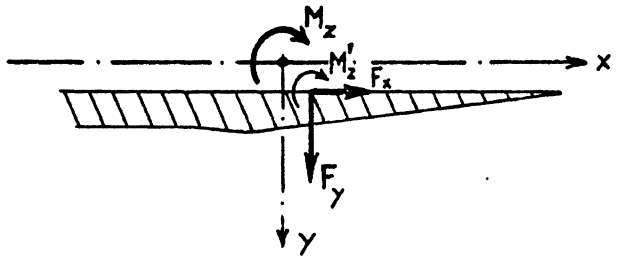

Figure 9. The base line of the tread elements translated according to simplified representation of carcass flexibility.

In the adhesion region we have :

$$q_x = k_x u, \qquad q_y = k_y v \tag{24}$$

with

$$u = u_a(a-x)/(a-x_a), \qquad v = v_a(a-x)/(a-x_a) \tag{25}$$

In the transition region we have:

$$q_x = k_x u, \qquad q_y = k_y v \tag{26}$$

with

$$u = [(x_a - x)u_s + (x - x_s)u_a]/t$$
$$v = [(x_a - x)v_s + (x - x_s)v_a]/t \tag{27}$$

In the steady state region we have:

$$q_x = -(V_{cx}/V_c)\mu q_z, \qquad q_y = -(V_{cy}/V_c)\mu q_z \tag{28}$$

Generally valid expressions for the forces and the moment may be derived after the introduction of the quantities defined below.

Variable	RANGE 1 (If Only Adhesion Region Occurs) $x_a \leq -a,\ x_s < -a$	RANGE 2 (If Also Transition Region Occurs) $x_a > -a,\ x_s < -a$	RANGE 3 (If Also Steady State Region Occurs) $x_a > -a,\ x_s \geq -a$
$x'_a =$	$-a$	x_a	x_a
$x'_s =$	$-a$	$-a$	x_s
$u'_a =$	$2a u_a/(a - x_a)$	u_a	u_a
$v'_a =$	$2a v_a/(a - x_a)$	v_a	v_a
$u'_s =$	0	$[(x_a + a)u_s - (x_s + a)u_a]/t$	u_s
$v'_s =$	0	$[(x_a + a)v_s - (x_s + a)v_a]/t$	v_s

(29)

We obtain sums over the adhesion, transition and steady state regions:

$$F_x = F_{xa} + F_{xt} + F_{xs} \tag{30}$$

$$F_y = F_{ya} + F_{yt} + F_{ys} \tag{31}$$

$$M_z = M_{za} + M_{zt} + M_{zs} + F_x F_y (1/K_x - 1/K_y) \tag{32}$$

where

$$F_{xa} = bk_x u'_a (a - x'_a) \tag{33}$$

$$F_{xt} = bk_x (u'_a + u'_s)(x'_a - x'_s) \tag{34}$$

$$F_{xs} = 2bk_x u'_s (a + x'_s) \tag{35}$$

$$F_{ya} = bk_y v'_a (a - x'_a) \tag{36}$$

$$F_{yt} = bk_y (v'_a + v'_s)(x'_a - x'_s) \tag{37}$$

$$F_{ys} = 2bk_y v'_s (a + x'_s) \tag{38}$$

The expressions for the moment are complicated and are not reproduced here.

For vanishing slip ($s'_x \to 0$ and $s'_y \to 0$) we may linearize and obtain the result for the case of complete adhesion:

$$F_x = -4a^2 bk_x s'_x = -C_s s'_x \simeq -C_s s_x = -C_s (V_{cx}/V_x) \tag{39}$$

$$F_y = -4a^2 bk_y s'_y = -C_\alpha s'_y \simeq -C_\alpha s_y = -C_\alpha \tan \alpha \tag{40}$$

$$M_z = (4/3)a^3 bk_y s'_y = C_{M\alpha} s'_y \simeq C_{M\alpha} s_y = C_{M\alpha} \tan \alpha \tag{41}$$

with C_s, C_α, and $C_{M\alpha}$ denoting the slip stiffnesses:

$$C_s = 4a^2 bk_x \tag{42}$$

$$C_\alpha = 4a^2 bk_y \tag{43}$$

$$C_{M\alpha} = \tfrac{4}{3} a^3 bk_y \tag{44}$$

COMPUTED CHARACTERISTICS

For the same parameter values of the tire model as employed in Ref. [1] the force and moment response to combined side and longitudinal slip has been calculated. In the subsequent Figures 10 through 13, two series of results are shown. The first (shown at the top of the page) for a relatively large longitudinal slip stiffness, C_s, and the second (bottom figure) for a relatively low value of C_s. The following parameter values were used:

$$V = 50 \text{ ft/sec}, \; A_s = 0.00353 \text{ sec/ft}, \; \mu_o = 0.53$$

$$C_\alpha = 10 \; |F_z| \text{ (lb/rad)}, \; C_s = 40 \; |F_z| \text{ or } 5 \; |F_z| \text{ (lb/unit slip)}$$

$$K_x = 4 \; |F_z|/a \text{(lb/ft)}, \; K_y = 2 \; |F_z|/a \text{(lb/ft)}$$

Note: the values of F_z and α are not relevant since the responses are computed and shown in the following non-dimensional form:

$$\overline{F}_x = F_x/|F_z|, \; \overline{F}_y = F_y/|F_z|, \; \overline{M}_z = M_z/(a|F_z|) \tag{45}$$

The calculated results are qualitatively similar to experimental findings. An important result is that according to this analysis, the difference in the F_y-α curves due to a variation in longitudinal slip stiffness, C_s, is insignificant. In the F_x-s_x diagrams the slope at the origin reduces in value due to a lower value of C_s. The F_y-F_x curves of Figure 12, calculated for s_x values varying from -2 to +1 (=wheel lock) at constant values of α, turn out to change their shape when C_s is varied. The end points at wheel lock remain at the same location, as should be expected. The moment M_z vs. α curves do not show the negative portion beyond a certain slip angle, as often occurs in practice. This discrepancy has been expected and is due to limitations of the model. The M_z-F_x curves show marked changes due to variations of C_s. The effect of introducing carcass compliance (finite K_x and K_y) is appreciable and the resulting M_z curves are qualitatively similar to experimental curves.

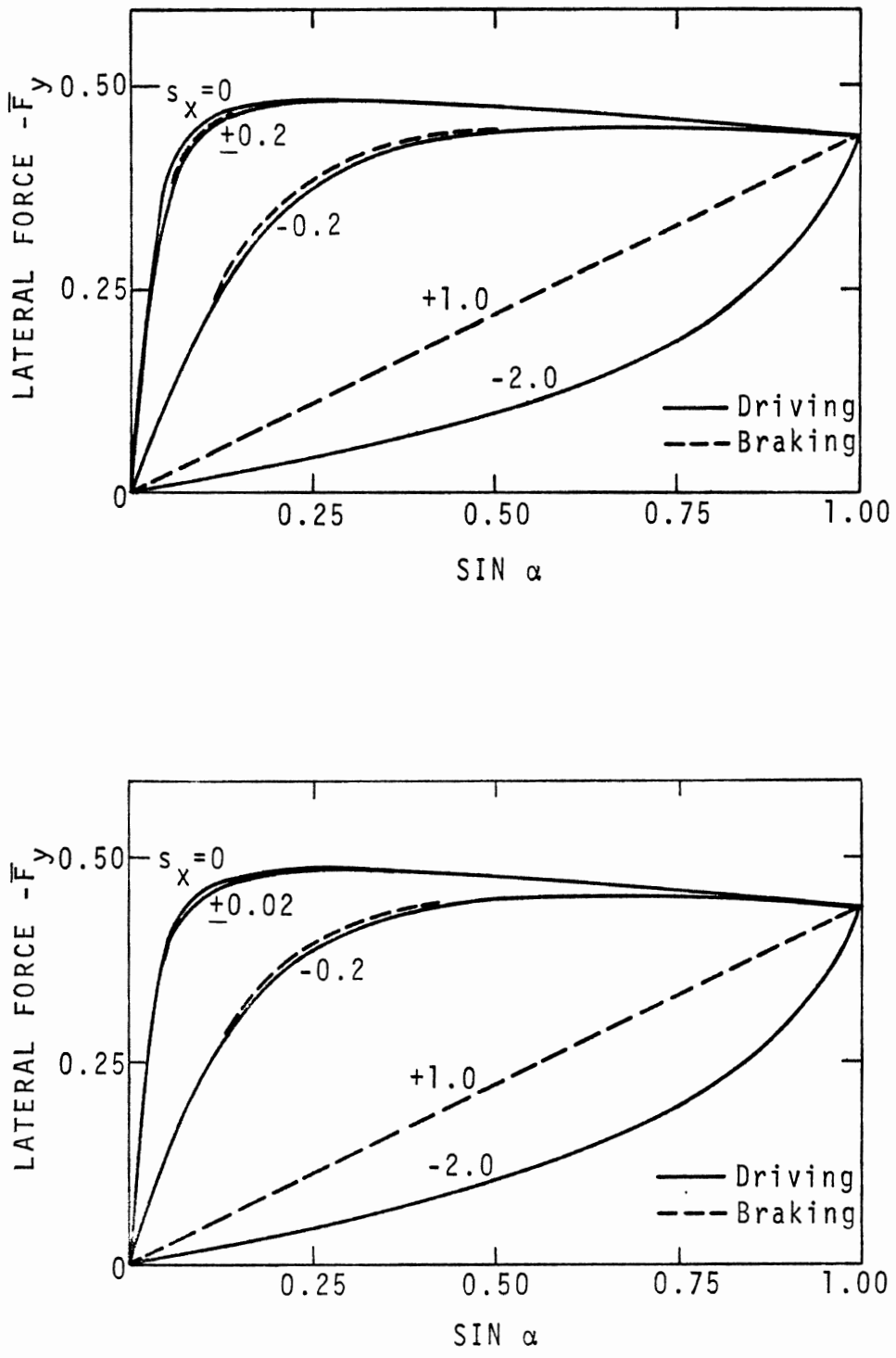

Figure 10. Side force as a function of slip angle, influenced by longitudinal slip s_x for longitudinal slip stiffness C_s equal to $40|F_z|$ (above) and $5|F_z|$ (below).

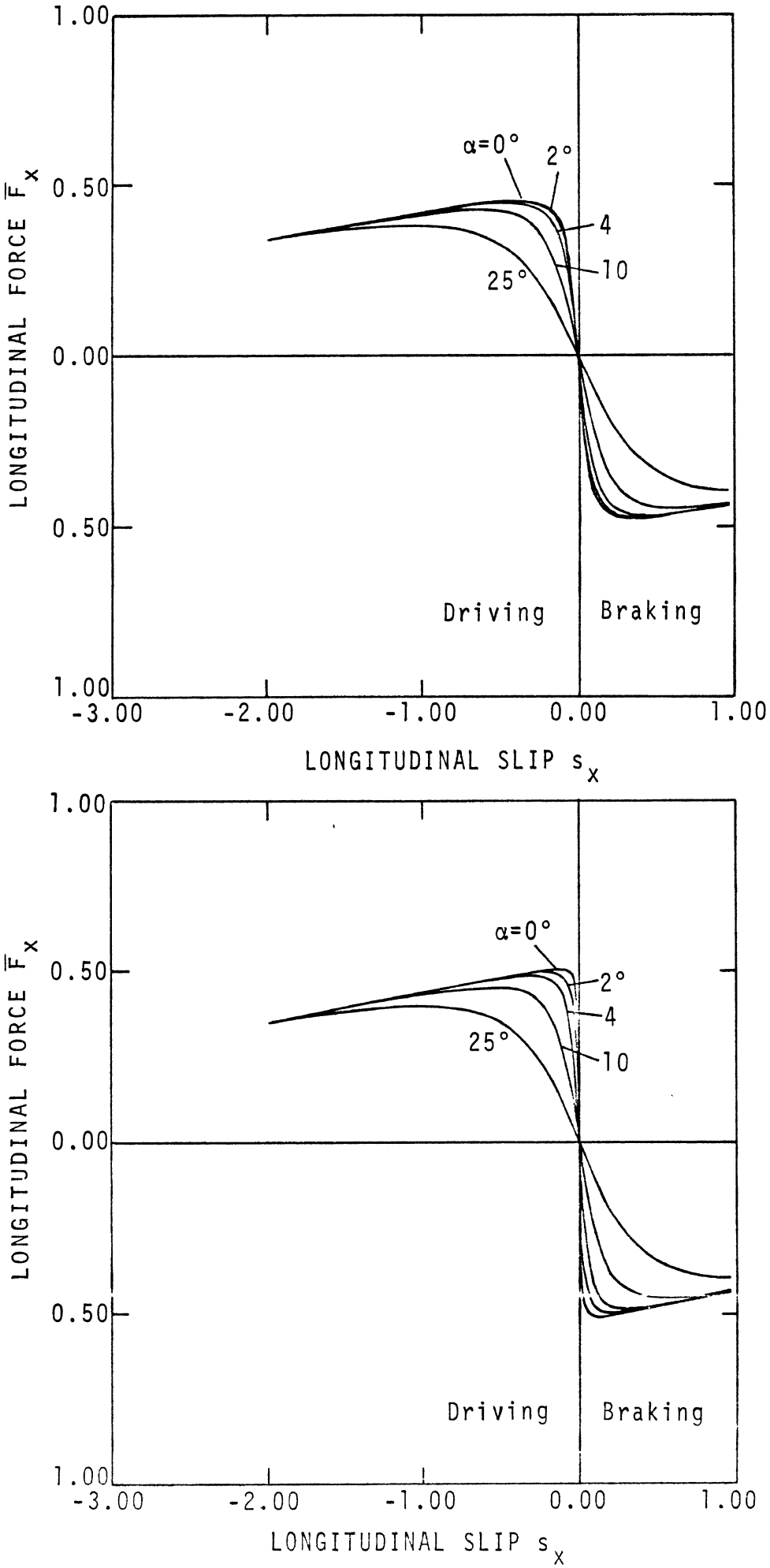

Figure 11. Longitudinal force as a function of longitudinal slip influenced by slip angle α for same parameters as Figure 10

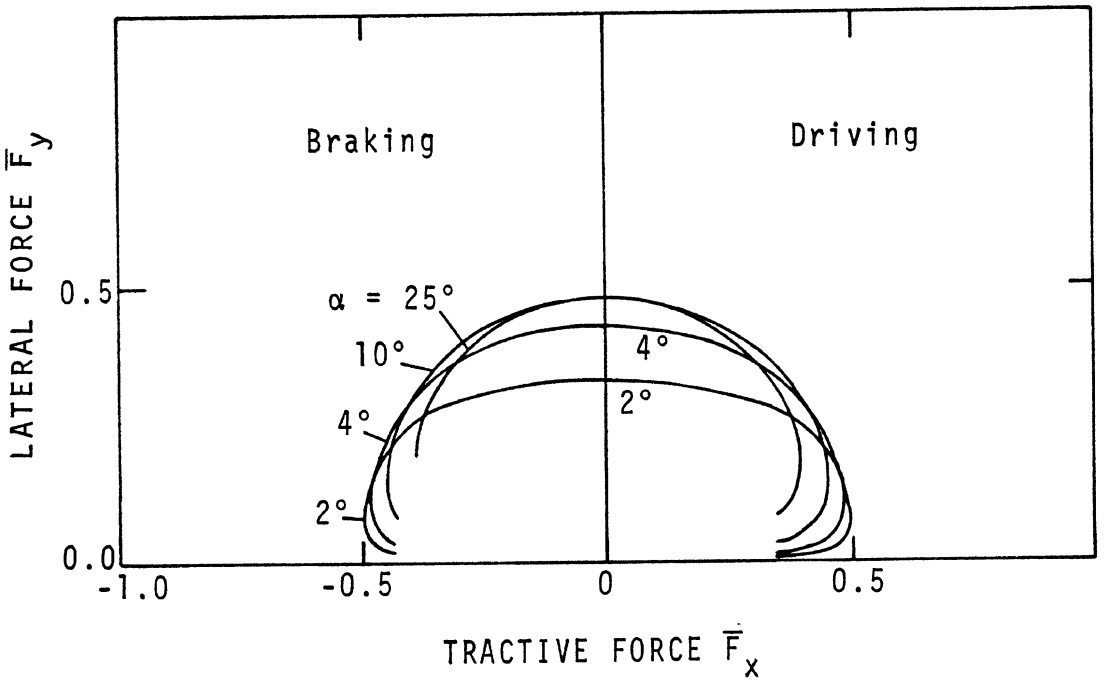

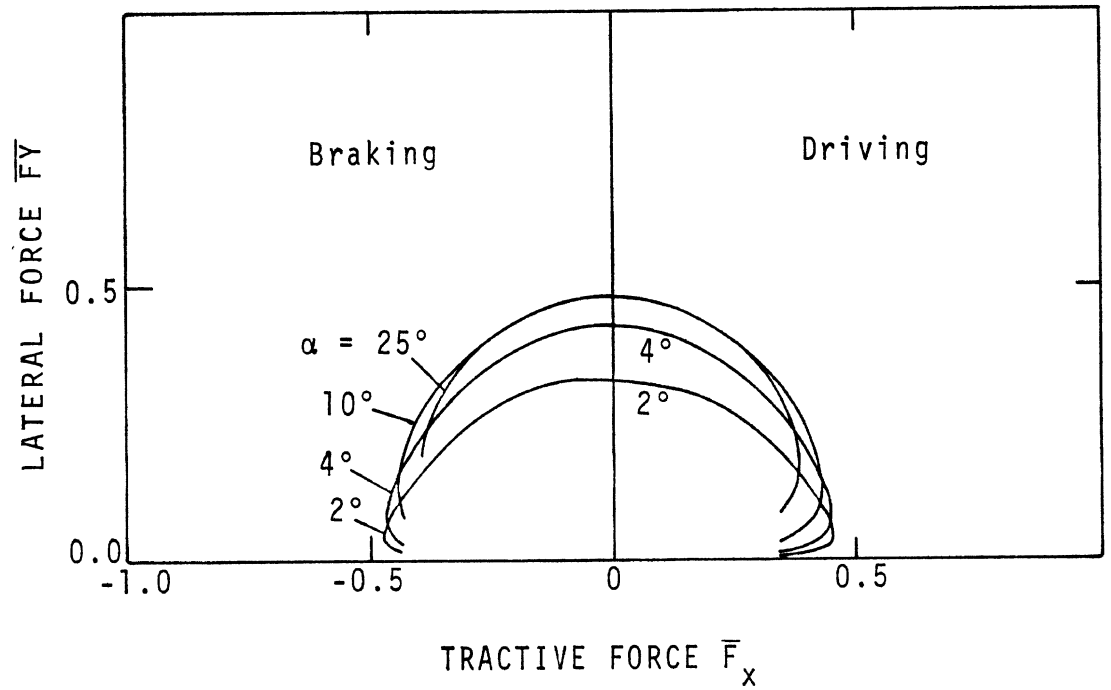

Figure 12. Lateral force as a function of longitudinal force for different values of slip angle. Same parameter values as in Figure 10.

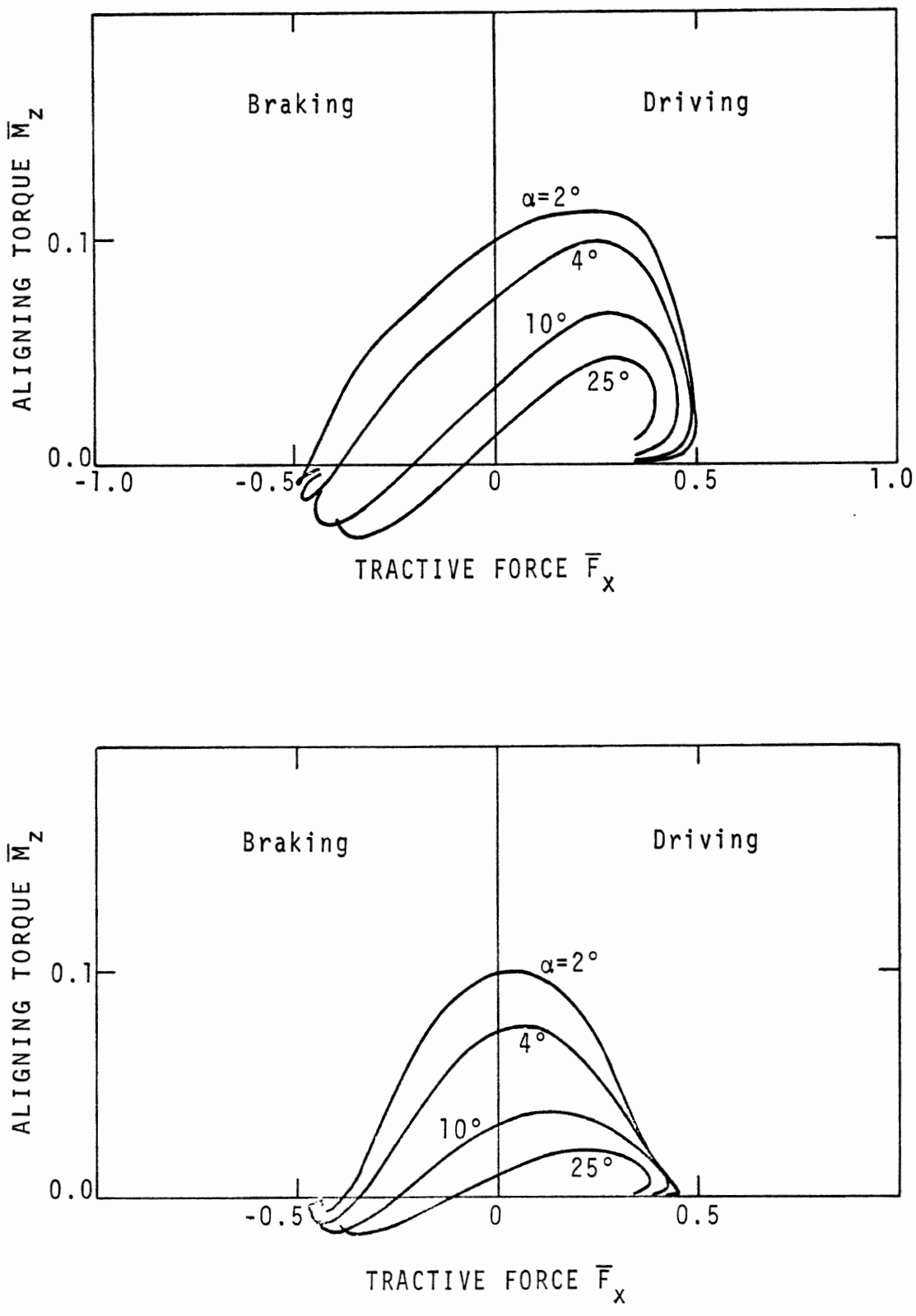

Figure 13. Aligning torque as a function of longitudinal force for different values of slip angle. Same parameter values as in Figure 10.

SECTION 2

SIMILARITY METHOD

The object of this method is to establish a mathematical description of tire shear force and aligning moment characteristics for any combination of longitudinal and lateral slip and of camber, at any vertical load and speed of travel, within ranges covered by experimental data. The method makes use of a set of measured characteristics for longitudinal force, F_x, lateral force, F_y, and aligning moment, Ω_z, as a function of slip angle, α, longitudinal slip, s, and camber angle, γ, at different values of vertical load, F_z, and velocity, V. From these data, basic curves and other basic relations are derived. In earlier work, the method was developed for the case of dry road contact and for longitudinal force rather than longitudinal slip as the input. The relations obtained are relatively simple (cf. Chap. 7.5 of Clark's Mechanics of Pneumatic Tires). In the following work, the behavior on wet roads, with highly sliding speed dependent shear forces, resulting in decaying characteristics for the forces versus slip, is generated by a set of mathematical formulations. It should be noted that this theory does not attempt to model the physics of tire behavior. It merely tries to describe mathematically the shear force generation of a tire based on measurements of this tire on a specific road under specific circumstances.

Wet Traction

On dry surfaces, where μ is less dependent on sliding speed than on wet surfaces, F_y may be a single valued function of F_x for a given slip angle, α. Experiments on wet surfaces show a different picture as illustrated on the following page:

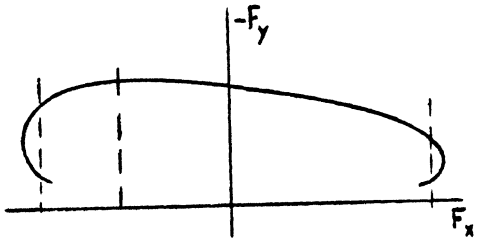

In order to cover the entire curve, we must adopt an input variable different from F_x. For this purpose, we choose the longitudinal slip, s, as the input variable. Its definition is:

$$s = 100 \cdot \frac{V_x - \Omega R_{eo}}{V_x} \quad (\%)$$

where V_x denotes the longitudinal speed component of the wheel center and Ω the revolving speed of the wheel about the spin axis and R_{eo} the effective rolling radius at free rolling. Obviously, s=0 at free rolling and is 100% when the wheel is locked. Under the action of driving forces s becomes negative.

An outline of the successive steps to be taken in order to arrive at the force and moment functions of variables α, s, γ and parameters V and F_z is given below.

Influence Speed V

1. Take the measured curves for (F_x-s) and (F_y-α) at nominal load ($-F_{z0}$) and for different speeds V. Introduce new slip notations: $s_x = \frac{s}{100}$, $s_y = \sin \alpha$.

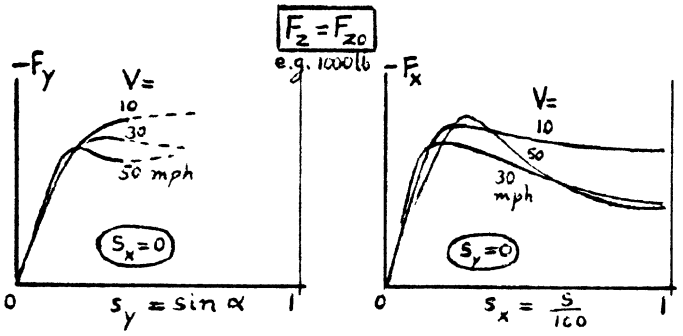

2. Transform these curves to basic curves F_{yB} and F_{xB} (one for F_y-α, one for F_x-s) so that by proper multiplication with factors, which are functions of V, the original curves are approximately obtained.

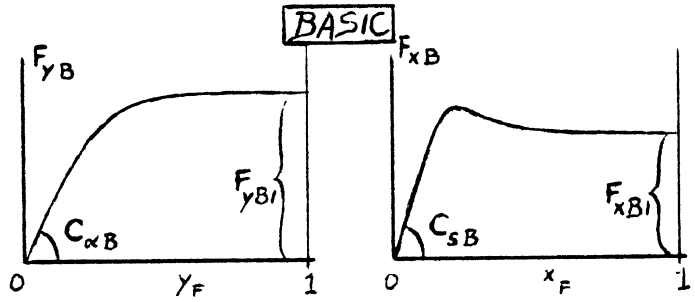

Three types of multiplication are required:

(1) vertical multiplication with a factor ϕ_V which approaches unity when $s \to 0$ and $\alpha \to 0$. This factor brings about the decay of the curves due to increasing sliding speeds without effecting the slope in the origin.

(2) radial multiplication with a factor λ_V being a function of V which causes a change in the total level of the curve.

(3) horizontal multiplication with a factor η_V being a function of V which brings about a change in slope at $s=0$ and $\alpha=0$.

The latter two multiplications may be applied to a range of the basic curves beyond sin α = 1 and s = 100%. In order to get proper results, the slope of the basic curves at s = 100% and sin α = 1 should be set equal or close to zero. The resulting formulae for F_x and F_y read:

$$-F_x = \phi_{xV} \cdot \lambda_{xV} \cdot F_{xB}(x_F) \qquad \text{with} \qquad x_F = \frac{\eta_{xV}}{\lambda_{xV}} \frac{s}{100} = \frac{\eta_{xV}}{\lambda_{xV}} s_x$$

$$-F_y = \phi_{yV} \cdot \lambda_{yV} \cdot F_{yB}(y_F) \qquad \text{with} \qquad y_F = \frac{\eta_{yV}}{\lambda_{yV}} \sin \alpha = \frac{\eta_{yV}}{\lambda_{yV}} s_y$$

(The actual functions for the different factors appearing in these equations are given on pages 24 and 25).

Influence Vertical Load $|F_z|$

3. Take the measured curves at nominal speed (V_o) and at different values of vertical load $|F_z|$.

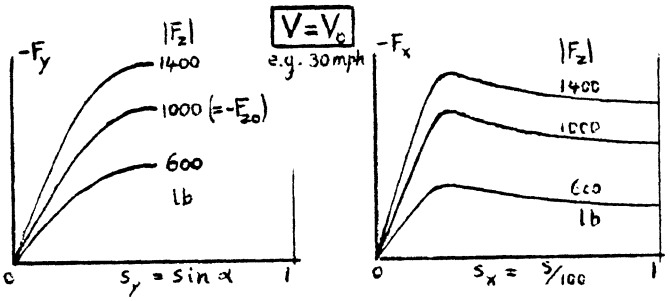

4. Transform the curves which are not measured under normal conditions (F_{z0}, V_o) to the curve for $F_z = F_{z0}$.

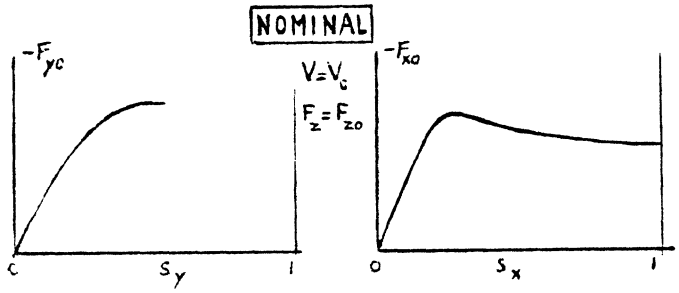

This may be done by successively multiplying in:

a) radial direction with a factor λ_F which changes the level without effecting the slope in the beginning. It has been observed (especially with the F_x curves) that the relative change in level is not only a function of F_z. Especially at high loads the factor may increase with slip. Therefore, λ_F will be a function of both load and slip. We may choose, for instance, a linear function for λ_{xF}:

$$\lambda_{xF} = (1 - s_x)\lambda_{xFo} + s_x\lambda_{xF1}$$

where factor λ_{xFo} takes care of the level at low slip values (near peak) and λ_{xF1} at values near the locked condition.

b) horizontal direction with factor η_F changing the slope at the origin as a function of vertical load.

At this stage, we have for the influences of V and $|F_z|$ combined:

$$-F_x = \phi_{xV} \cdot \lambda_x \cdot F_{xB}(x_F) \quad \text{with} \quad x_F = \frac{\eta_x}{\lambda_x} s_x$$

$$-F_y = \phi_{yV} \cdot \lambda_y \cdot F_{yB}(y_F) \quad \text{with} \quad y_F = \frac{\eta_y}{\lambda_y} s_y$$

where $\lambda_x = \lambda_{xV} \cdot \lambda_{xF}$, $\lambda_y = \lambda_{yV} \cdot \lambda_{yF}$

$$\eta_x = \eta_{xV} \cdot \eta_{xF} \quad , \quad \eta_y = \eta_{yV} \cdot \eta_{yF}$$

A possible interaction between V and $|F_z|$ has obviously been disregarded. It is therefore important that the nominal conditions V_o, $|F_{zo}|$ are close to the average operating conditions of the simulation.

Influence Small Camber Angles γ

5. Take the camber force characteristics for different speeds V and loads $|F_z|$. Determine the camber stiffness C_γ as a function of V and F_z.

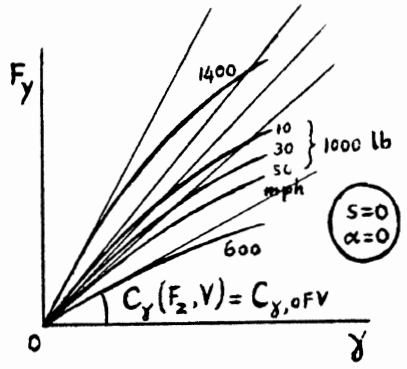

The camber stiffness may be taken as a product of a function of only the load and a function of only the speed.

$$C_\gamma = C_{\gamma,oFV} = C_{\gamma,oFo}(F_z) \cdot C_{\gamma,ooV}(V)/C_{\gamma,ooo}$$

6. Shift the $F_y(\alpha)$ curves found in 4 over the distance (to the right)

$$\Delta\alpha_F = \frac{C_\gamma}{C_\alpha} \gamma$$

which gives rise to the equivalent slip angle

$$\alpha_{eq} = \alpha - \frac{C_\gamma}{C_\alpha} \gamma \quad .$$

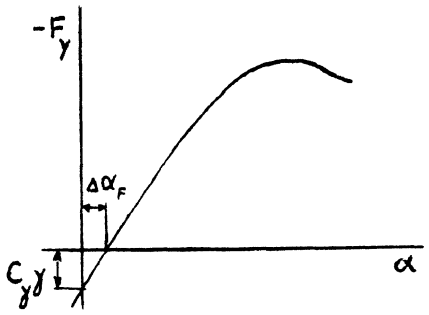

The cornering stiffness C_α follows from the slope of the basic curve $C_{\alpha B}$ by multiplication with factor η_y

$$C_\alpha = \eta_y C_{\alpha B}$$

The argument y_F reads now:

$$y_F = \frac{\eta_y}{\lambda_y} \sin(\alpha - \frac{C_\gamma}{C_\alpha} \gamma) = \frac{\eta_y}{\lambda_y} \bar{s}_y$$

with the equivalent sideslip:

$$\bar{s}_y = \sin \alpha_{eq}$$

Interaction Longitudinal and Lateral Slip

7. The complicated interaction process of longitudinal and lateral slip is a difficult matter. A more or less precise generation of the forces as a function of s_y and s_x would require a large number of manipulations. A relatively simple representation which appears to work satisfactorily will be given here. Use will be made of the curves at (V, F_z) as computed before for either pure s_y or pure s_x (see the figure on the following page).

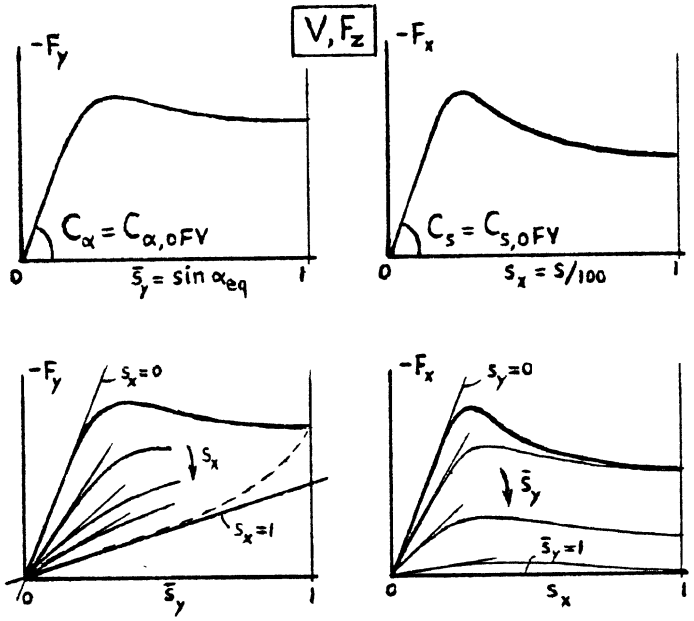

Next, the variation of the initial slope due to interacting slip is taken into account. The corresponding stiffnesses $C_{\alpha,sFV}$ and $C_{s,\alpha FV}$ may be found from the measured variation of these stiffnesses at nominal speed V_o and load F_{zo}. The latter stiffnesses are denoted by $C_{\alpha,soo}$ and $C_{s,\alpha oo}$. The variations of these quantities with slip are as shown below. (The actual curves derived from the initial slopes of measured characteristics should be determined very carefully.)

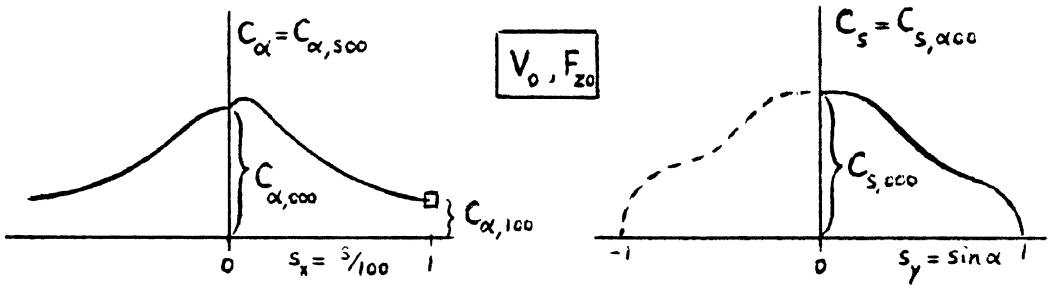

The stiffnesses under different conditions may approximately be obtained by considering the changes which occur with C_α at s=0 and 100% and with C_s at α=0. (The value of C_s will tend to zero for sin α = 1, anyway.) A multiplication factor η_{ys} for C_α which varies linearly with s_x is employed so that the experimentally found changes with F_z and V are fulfilled at s=0 and 100%. A factor $\eta_{x\alpha}$ is employed for representing the changes in C_s.

$$\eta_{ys} = \eta_{yso}(1 - s_x) + \eta_{ys1}s_x \; ; \quad \eta_{x\alpha} = \frac{C_{s,oFV}}{C_{s,ooo}}$$

with $$\eta_{yso} = \frac{C_{\alpha,oFV}}{C_{\alpha,ooo}} \quad \text{and} \quad \eta_{ys1} = \frac{C_{\alpha,1FV}}{C_{\alpha,1oo}}$$

where $C_{\alpha,oFV}$ and $C_{s,oFV}$ and $C_{\alpha,1FV}$ are functions of F_z and V. They may be approximated by a product of a function of F_z and a function of V. From before

$$C_{\alpha,sFV} = \eta_{ys} \cdot C_{\alpha,soo} \; ; \quad C_{s,\alpha FV} = \eta_{x\alpha} \cdot C_{s,\alpha oo}$$

The indices after the comma denote the values of the slip $s_{x,y}$ (o=zero), the load (o=nominal) and the speed (o=nominal), respectively. After the slip stiffnesses have been established, the (F_x - s_x) and (F_y - s_y) diagrams will be multiplied in vertical direction in such a way that the initial slope produces the required stiffness. Moreover, the F_y curve should approach a straight line with slope representing the stiffness $C_{\alpha,1FV}$ at s_x=1. The F_x curves approach the abscissa at $s_y \to 1$. In case of the F_x curves, the multiplication factor should be taken as a function of s_x. In general, it appears that the multiplication factor ($\phi_{x\alpha}$) is a strongly nonlinear function of s_x which may be sufficiently represented by a fourth degree function of s_x. (See figure below.) For the multiplication factor of the F_y curve, we did not attempt to make it a function of α as only relatively small values of s_y = sin α are considered.

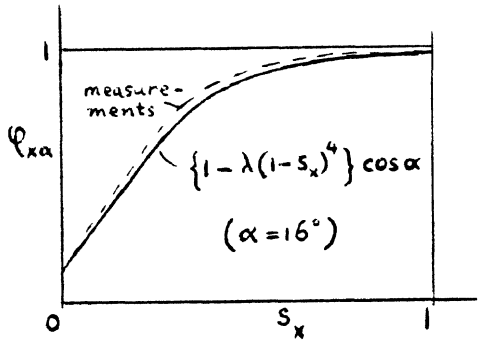

The multiplication factors, finally, will have the following form:

$$\phi_{ys} = \frac{C_{\alpha,sFV} - C_{\alpha,1FV}}{C_{\alpha,oFV} - C_{\alpha,1FV}}$$

$$\phi_{x\alpha} = \left[1 - \frac{C_{s,oFV} \cos \alpha_{eq} - C_{s,\alpha FV}}{C_{s,oFV} \cos \alpha_{eq}} (1-s_x)^4\right] \cos \alpha_{eq}$$

How these factors are used in the final equations is shown in the following.

Complete Functions for F_x and F_y

8. The proposed final equations for F_x and F_y as influenced by F_z, V, s and α read:

$$\left.\begin{aligned} -F_y &= \phi_{ys}\ \phi_{yV}\ \lambda_{yV}\ \lambda_{yF} F_{yB}(y_F) + C_{\alpha,1FV}\ \bar{s}_y(1-\phi_{ys}) \\ -F_x &= \phi_{x\alpha}\ \phi_{xV}\ \lambda_{xV}\ \lambda_{xF} F_{xB}(x_F) \end{aligned}\right\} \quad (1)$$

with

$F_{yB}(y_F)$ = basic function of y_F $\quad$ $F_{xB}(x_F)$ = basic function of x_F

$$\left.\begin{array}{ll} y_F = \beta_y \text{ if } |\beta_y| \le 1 & x_F = \beta_x \text{ if } |\beta_x| \le 1 \\ y_F = \operatorname{sgn}\beta_y \text{ if } |\beta_y| > 1 & x_F = \operatorname{sgn}\beta_x \text{ if } |\beta_x| > 1 \\ \beta_y = \dfrac{\eta_{yV} \cdot \eta_{yF}}{\lambda_{yV} \cdot \lambda_{yF}} \bar{s}_y & \beta_x = \dfrac{\eta_{xV} \cdot \eta_{xF}}{\lambda_{xV} \cdot \lambda_{xF}} s_x \end{array}\right\} (2)$$

and

$$\phi_{ys} = \frac{C_{\alpha,sFV} - C_{\alpha,1FV}}{C_{\alpha,oFV} - C_{\alpha,1FV}} \qquad \phi_{x\alpha} = 1 - \frac{C_{s,oFV}\cos\alpha_{eq} - C_{s,FV}}{C_{s,oFV}\cos\alpha_{eq}}(1-s_x)^4 \cos\alpha_{eq}$$

$$\phi_{yV} = 1 - A_{sy}b_yV + B_{sy}b_y^2V^2 \qquad \phi_{xV} = 1 - A_{sx}b_xV + B_{sx}b_x^2V^2$$

$$b_y = \frac{1}{2}\left(\left|\,|\bar{s}_y| - s_{yV}\right| + |\bar{s}_y| - s_{yV}\right) \qquad b_x = \frac{1}{2}\left(\left|\,|s_x| - s_{xV}\right| + |s_x| - s_{xV}\right) \quad (3)$$

$$\bar{s}_y = \sin\alpha_{eq}\,,\ s_{yV} = \sin\alpha_V \qquad s_x = \frac{s}{100}\,,\ s_{xV} = \frac{s_V}{100}$$

$$\alpha_{eq} = \alpha - \gamma\ C_{\gamma,oFV}/C_{\alpha,oFV}$$

Note: s_{xV} and s_{yV} are illustrated in the figure on page 28.

$$\lambda_{yV} = \lambda_{yV}(V) \qquad \lambda_{xV} = \lambda_{xV}(V)$$

$$\lambda_{yF} = (1-s_y)\lambda_{yFo} + s_y\lambda_{yF1} \qquad \lambda_{xF} = (1-s_x)\lambda_{xFo} + s_x\lambda_{xF1}$$

$$\lambda_{yFo} = \lambda_{yFo}(F_z),\ \lambda_{yF1} = \lambda_{yF1}(F_z) \qquad \lambda_{xFo} = \lambda_{xFo}(F_z),\ \lambda_{xF1} = \lambda_{xF1}(F_z)$$

$$\eta_{yV} = C_{\alpha,ooV}/C_{\alpha B}, \qquad \eta_{xV} = C_{s,ooV}/C_{sB},$$

$$\eta_{yF} = C_{\alpha,oFo}/C_{\alpha,ooo} \qquad \eta_{xF} = C_{s,oFo}/C_{s,ooo}$$

The various slip stiffnesses are found as follows:

$$C_{\alpha,oFV} = \frac{C_{\alpha,oFo} \cdot C_{\alpha,ooV}}{C_{\alpha,ooo}} \qquad C_{s,oFV} = \frac{C_{s,oFo} \cdot C_{s,ooV}}{C_{s,ooo}}$$

$$= \eta_{yF}\eta_{yV}C_{\alpha B} \qquad = \eta_{xF}\eta_{xV}C_{sB}$$

$$C_{\alpha,1FV} = \frac{C_{\alpha,1Fo}\ C_{\alpha,1oV}}{C_{\alpha,1oo}}$$

$$C_{\alpha,sFV} = \eta_{ys} \cdot C_{\alpha,soo} \qquad C_{s,\alpha FV} = \eta_{x\alpha} \cdot C_{s,\alpha oo} \qquad (4)$$

$$\eta_{ys} = \eta_{yso}(1-s_x) + \eta_{ys1}s_x \qquad \eta_{x\alpha} = C_{s,oFV}/C_{s,ooo}$$

$$\eta_{yso} = C_{\alpha,oFV}/C_{\alpha,ooo},\ \eta_{ys1} = C_{\alpha,1FV}/C_{\alpha,1oo}$$

$$C_{\gamma,oFV} = \frac{C_{\gamma,oFo} \cdot C_{\gamma,ooV}}{C_{\gamma,ooo}}$$

PROCEDURES

For the mathematical description of shear force generation (Eqs. (1), (2), (3), (4)) to be useful, it must be applied to the measured characteristics of an actual tire. A proposed way to arrive at the final equations is given below.

General Force Functions

$$-F_y = \phi_{ys}\phi_{yV}\lambda_{yV}\lambda_{yF}F_{yB}(y_F) + C_{\alpha,1FV}\bar{s}_y(1-\psi_{ys})$$

$$-F_x = \phi_{x\alpha}\phi_{xV}\lambda_{xV}\lambda_{xF}F_{xB}(x_F)$$

Arguments

$$\beta_y = \frac{\eta_{yV} \cdot \eta_{yF}}{\lambda_{yV} \cdot \lambda_{yF}} \bar{s}_y \qquad \beta_x = \frac{\eta_{xV} \cdot \eta_{xF}}{\lambda_{xV} \cdot \lambda_{xF}} s_x$$

$$\left.\begin{aligned} y_F &= \beta_y \quad \text{if} \quad |\beta_y| \leq 1 \\ y_F &= \operatorname{sgn} \beta_y \quad \text{if} \quad |\beta_y| > 1 \end{aligned}\right\}$$

$$\left.\begin{aligned} x_F &= \beta_x \quad \text{if} \quad |\beta_x| \leq 1 \\ x_F &= \operatorname{sgn} \beta_x \quad \text{if} \quad |\beta_x| > 1 \end{aligned}\right\}$$

The various subfunctions appearing in these shear force formulae are found in successive steps starting with the original curves for different V and nominal load $|F_z|$.

1. First construct the basic curve F_B by extrapolating the V-curves to a curve which would hold for a speed V=0. Then (if necessary) multiply the V→0 curve with a factor in horizontal direction so that its slope at the origin becomes equal or almost equal to the slope of the steepest curve. We call the curve thus obtained the basic curve F_B which, through the above manipulation, will not need to extend beyond a slip value equal to one.

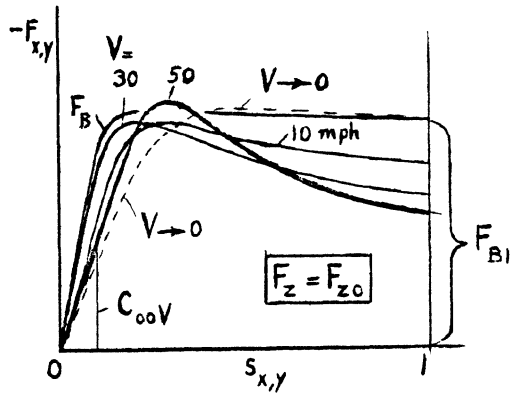

The slope at the origin of the basic curve is given by the slip stiffness C_B. The stiffnesses of the other (V) curves are designated with C_{ooV}. (Note that suffixes s, y, α and s have been omitted here.)

2. Replace original V-curves by curves which deviate from them at larger slip values in that the tendency to end in a concave manner is absent. The new curves should tend to inclined straight assymptotes of which the slope (ε) preferably changes linearly with V. The deviation (Δ) of the original curves from the assymptotes should preferably vary quadratically with V.

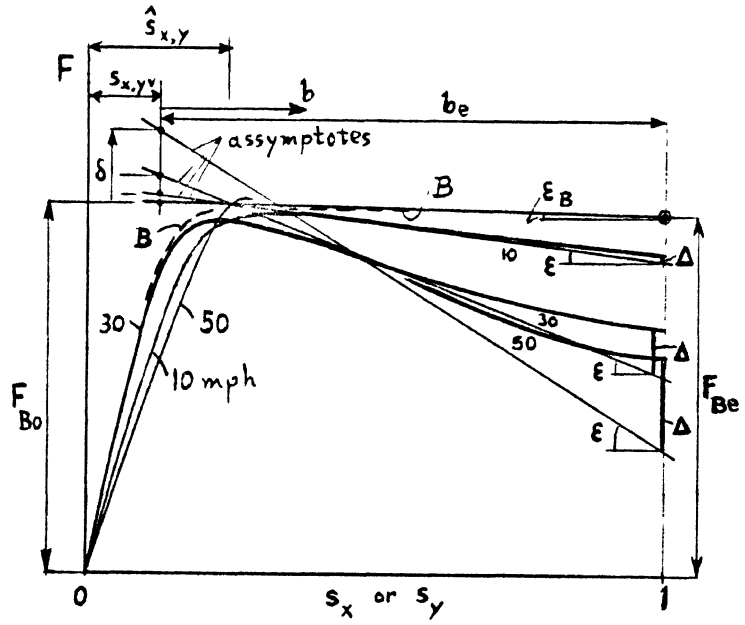

The slope of the assymptote of the basic curve should be zero or small. Determine the slip value where the top of the nominal curve (V=30 mph) is reached. Half this value is called s_V and α_V. Draw a vertical line through $\alpha = \alpha_V$ and $s = s_V$. All the assymptotes intersect this vertical line at different distances δ above the point of intersection of the B-assymptote with the vertical line. This latter point is located a distance F_{Bo} above the horizontal axis.

The original V curves may be approximately obtained from the basic curve (B) by first multiplying B with a factor $\frac{1}{\eta_V} = \frac{C_B}{C_{ooV}}$ in horizontal direction so that the slopes at 0 coincide. Then multiplying with factor $\lambda_V = (F_{Bo} + \delta)/F_{Bo}$ in radial direction so that the slope doesn't change but the level of the point of intersection of assymptote and vertical line is made approximately equal to the level of that point of the V-curve. Finally, multiplying with the δ_V factor which must be equal to 1 for

vanishing slip values (α or s) and further must produce the slope which (linearly) varies with V and the concave portion which (quadratically) varies with V. The value 1 is realized by assuming that the deviation from the B-curve due to this ϕ_V factor starts only at a slip value halfway to the value where the nominal curve becomes maximum. (This is an assumption which may be close to reality as the influence of sliding speed, which ϕ_V tries to express, only starts to act over the entire contact patch when full sliding begins, which assumedly occurs near the top of the curve.)

$$\phi_V = 1 - A_s V b + B_s V^2 b^2 \text{ for } |b| \geq 0 \text{ or } \phi_V = 1 \text{ for } |b| < 0$$

with b the |slip value| minus the halfway value: $b = |s_{x,y}| - s_{x,yv}$. The value of A_s follows from the slope $\varepsilon (\simeq A_s V + \varepsilon_B)$; B_s follows from deviation $\Delta (\simeq B_s V^2 b_e^2 F_{Be} \lambda_V)$ at $b=b_e$ (see Figure on page 28). The factors A_s and B_s are here treated as constants. The factors η_V and λ_V may be given an appropriate functional relationship with V.

3. The changes in slip stiffnesses C_α, C_s due to vertical load variations are expressed by the factors η_F. This factor is defined as the ratio between the slip stiffness at certain $|F_z|$ and the slip stiffness at nominal load $|F_{zo}|$ both at nominal speed V_o.

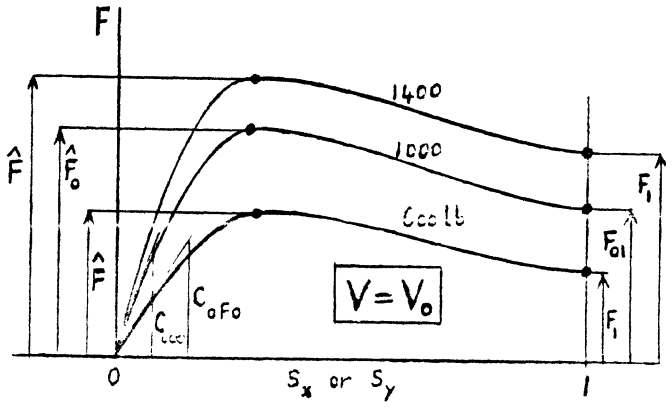

$$\eta_F = \frac{C_{oFo}}{C_{ooo}}$$

Through horizontal multiplication of the original curves with this factor, all the slopes become equal at zero slip. By subsequent multiplication with factor λ_F in radial direction, the level of the top (at relatively small slip values, $\lambda_F = \lambda_{Fo}$) and at large values of slip near 1 where the curves have an almost horizontal tangent ($\lambda_F = \lambda_{F1}$) can be attained approximately. We have

$$\lambda_{Fo} = \frac{\hat{F}}{F_o} \quad , \qquad \lambda_{F1} = \frac{F_1}{F_{o1}}$$

where $\hat{F}$ and F_1 depend on $|F_z|$. Some functional relationship of η_F, λ_{Fo} and λ_{F1} with F_z may be established.

4. The interaction of slip is mainly determined by the factors ϕ_{ys} and $\phi_{x\alpha}$. These factors reduce the portion of the F value that is left after subtracting from the original curves $-F_{y,x}$ the linear functions $C_{\alpha,1FV} \cdot \bar{s}_y$ and $C_{s,1FV}\, s_x$ (=0), respectively. The formulae given before indicate how the factors are determined.

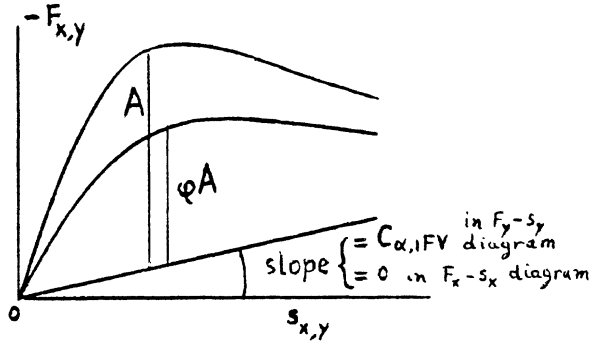

The functions $C_{\alpha,soo}$ and $C_{s,\alpha oo}$ result from the original interaction curves at nominal speed and load (F_{zo}, V_o). The slope variation of the F_x vs. s_x curves at the origin yields the function $C_{s,\alpha oo}(s_y)$. The initial slope of the constructed F_y vs. s_y curves for various fixed values of s_x serves for the determination of the function $C_{\alpha,soo}(s_x)$. For $\alpha \to 90°$ ($s_y \to 1$) we have $C_{s,\alpha oo} \to 0$. For $s \to 100\%$ ($s_x \to 1$) we have $C_{\alpha,soo} = C_{\alpha,1oo}$.

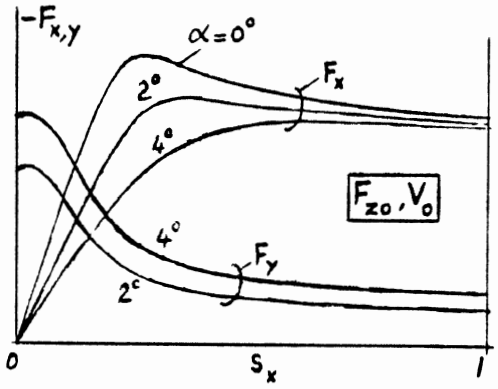

The functions $C_{\alpha,1Fo}(F_z)$ and $C_{\alpha,1oV}(V)$ may be obtained from the values of the original F_y interaction characteristics at $s_x = 1$ (wheel-lock) for different values of α, $|F_z|$ and V (see Figure).

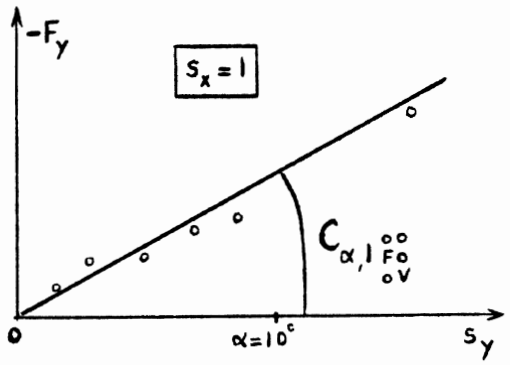

Application

The method as described before has been applied to the H-5 tire on wet asphalt. In graphs I, II and III the original F_y and F_x curves are given for different speed V and load $|F_z|$. In the graphs I and II the basic F_B curves are shown. In graph I we arrive at F_{yB} by extrapolation. The differences in slope at 0 are small so that a horizontal multiplication does not seem necessary, since we are interested only in relatively small slip angles (< 20°). However, this was needed in graph II for F_x. There, the F_{xB} curve should extend beyond s_x=1 if, for instance, the curve for V=30 mph is to be derived from the basic F_{xB} curve. In order to save space,

we have multiplied the F_{xB} curve with a certain factor so that its slope equals the slope of the 30 mph curve. To determine the position of the "assymptotes" in order to have their slope vary linearly with V and their deviation from the original curves at high slip values (shaded area) change quadratically with V, is really more an art than a science. We expect that the simulated curves will be all right at small slip values and at large slip values. The transition range may show deviations in curvature. For instance, the F_y curve at 50 mph shows a relatively sharp curvature near its maximum value. It seems impossible to derive such a curvature from the relatively smooth basic curve. The same may hold for the 50 mph F_x curve. However, it would not be surprising if the error lies within the range of inaccuracy of the measurements. In order to be able to describe the deviation from the assymptotes at s_x=1 (s=100%) (Graph II) in terms of V^2, the 30 mph curve was replaced by the shown substitutive curve.

The approximate functional relationships for C_{ooV} and λ_V are shown in Graphs I and II.

Graphs I and III show the influence of changing the vertical load. As the F_y values are given only for relatively small slip values (s_y), it is sufficient to use a λ_{yF} for small and for large values of s_x. The λ_{xFo} (small s_x, near peak) and the λ_{xF1} (at s_x=1) obtained are shown graphically. Also, the variation of the slip stiffness $C_{\alpha,oFo}$ with $|F_z|$ at $V=V_o$=30 mph is shown.

In Graph IV, the measured interaction-curves have been shown. The solid straight lines are tangents to the F_x-curves in the origin. From them we obtain $C_{s,\alpha oo}(\alpha)$ as shown in Graph V. The dashed curves in Graph IV are F_y-α curves for different values of slip % (indicated at origin of dashed curves). They are obtained from the F_y-s curves. From the tangents to the dashed curves at their origins, we obtain the $C_{\alpha,soo}(s)$ values shown in the same Graph V. In Graph IV, also, the F_y values at s_x=1 for different values of

load and speed are shown. From these data we find $C_{\alpha,1oV}(V)$ and $C_{\alpha,1Fo}(F_z)$.

A collection of formulae and constant values are listed on the next pages. The functions $F_{xB}(x_F)$, $F_{yB}(y_F)$ are shown on Graph VI.

Calculations have been carried out in order to check the validity of the method. For a number of combinations of α values (2° and 16°), s values (10%, 30%, 70%) and V values (30 mph and 50 mph) the results are shown on the last two diagrams VII and VIII in comparison with the original measured curves. A reasonable agreement appears to occur. A better choice of constants may give rise to results which are closer to the experimental data.

Sub-Functions (For main functions, see formulae (1) and (2) on pages 23 and 24).

(V in mph, $C_{\alpha,...}$ in lbs/rad, $C_{s,...}$ in lbs/-, $F_{...}$ in lbs)

$$f_z = - 10^{-3} F_z$$

$$\phi_{yV} = 1 - A_{sy}Vb_y + B_{sy}V^2b_y^2 \qquad \phi_{xV} = 1 - A_{sx}Vb_x + B_{sx}V^2b_x^2$$

$$b_y = \frac{1}{2}\left(\left||\bar{s}_y| - s_{yV}\right| + |s_y| - s_{yV}\right) \qquad b_x = \frac{1}{2}\left(\left||s_x| - s_{xV}\right| + |s_x| - s_{xV}\right)$$

$$F_y = \sin \alpha_{eq}\ , \quad s_{yV} = \sin \alpha_y \qquad s_x = \frac{s}{100}\ , \quad s_{xV} = \frac{s_V}{100}$$

$$\alpha_{eq} = \alpha - \gamma C_{\gamma,oFV}/C_{\alpha,oFV}$$

$$\lambda_{yV} = 1 + 8 \times 10^{-4}V$$

$$\lambda_{yF} = 1.04\, f_z - 0.184(|f_z-0.9| + f_z-0.9)$$

$$\lambda_{xV} = 1 + 3.6 \times 10^{-5}(V-10)^2$$

$$\lambda_{xF} = (1-s_x)\lambda_{xFo} + s_x\lambda_{xF1}$$

$$\lambda_{xFo} = f_z-0.182s(|f_z-1| + f_z-1)$$

$$\lambda_{xF1} = 1.085f_z-0.116(|f_z-0.6| + f_z-0.6)$$

$$\eta_{yV} = C_{\alpha,ooV}/C_{\alpha B}$$

$$\eta_{yF} = C_{\alpha,oFo}/C_{\alpha,ooo}$$

$$\eta_{ys} = \eta_{yso}(1-s_x) + \eta_{ys1}s_x$$

$$\eta_{yso} = C_{\alpha,oFV}/C_{\alpha,ooo}$$

$$\eta_{ys1} = C_{\alpha,1FV}/C_{\alpha,1oo}$$

$$\phi_{ys} = \frac{C_{\alpha,sFV} - C_{\alpha,1FV}}{C_{\alpha,oFV} - C_{\alpha,1FV}}$$

$$C_{\alpha,oFV} = \eta_{yF}\eta_{yV}C_{\alpha B}$$

$$C_{\alpha,1FV} = C_{\alpha,1Fo} \cdot C_{\alpha,\,1oV}/C_{\alpha,ooo}$$

$$C_{\alpha,sFV} = \eta_{ys} \cdot C_{\alpha,soo}$$

$$C_{\gamma,oFV} = C_{\gamma,oFo} \cdot C_{\gamma,ooV}/C_{\gamma,ooo}$$

$$\eta_{xV} = C_{s,ooV}/C_{sB}$$

$$\eta_{xF} = C_{s,oFo}/C_{s,ooo}$$

$$\eta_{x\alpha} = C_{s,oFV}/C_{s,ooo}$$

$$\phi_{x\alpha} = \left\{1 - \frac{C_{s,oFV}\cos\alpha_{eq} - C_{s,\alpha FV}}{C_{s,oFV}\cos\alpha_{eq}}(1-s_x)^4\right\}\cos\alpha_{eq}$$

$$C_{s,oFV} = \eta_{xF}\eta_{xV}C_{sB}$$

$$C_{s,\alpha FV} = \eta_{x\alpha} \cdot C_{s,\alpha oo}$$

$C_{\alpha,ooV} = \frac{180}{\pi} 140\{1.1 - (V-34)^2 10.4 \times 10^{-5}\}$ $C_{s,ooV} = 16(6+V)(62-V)$

$C_{\alpha,oFo} = \frac{180}{\pi} \{157 - 119(f_z - 1.15)^2\}$ $C_{s,oFo} = 22700\ f_z(1-0.189f_z)$

$C_{\alpha,1oV} = 425 + 3V$

$C_{\alpha,1Fo} = 515\ f_z$

$C_{\gamma,ooV} = 1000\ f_z$

$C_{\gamma,oFo} = 1000\ f_z$

$C_{\alpha,soo} = C_{\alpha,soo}(s_x)$ $C_{s,\alpha oo} = C_{s,\alpha oo}(\bar{s}_y)$

Constants

$A_{sy} = 0.0235$ $A_{sx} = 0.021$

$B_{sy} = 0.00072$ $B_{sx} = 0.00026$

$\alpha_v = 4° \rightarrow s_{yV} = 0.07$ $s_v = 5\% \rightarrow s_{xV} = 0.05$

$C_{\alpha B} = 8000$ $C_{sB} = 18400$

$C_{\alpha,ooo} = 8850$ $C_{s,ooo} = 18400$

$C_{\alpha,1oo} = 515$

$C_{\gamma,ooo} = 1000\ f_z$

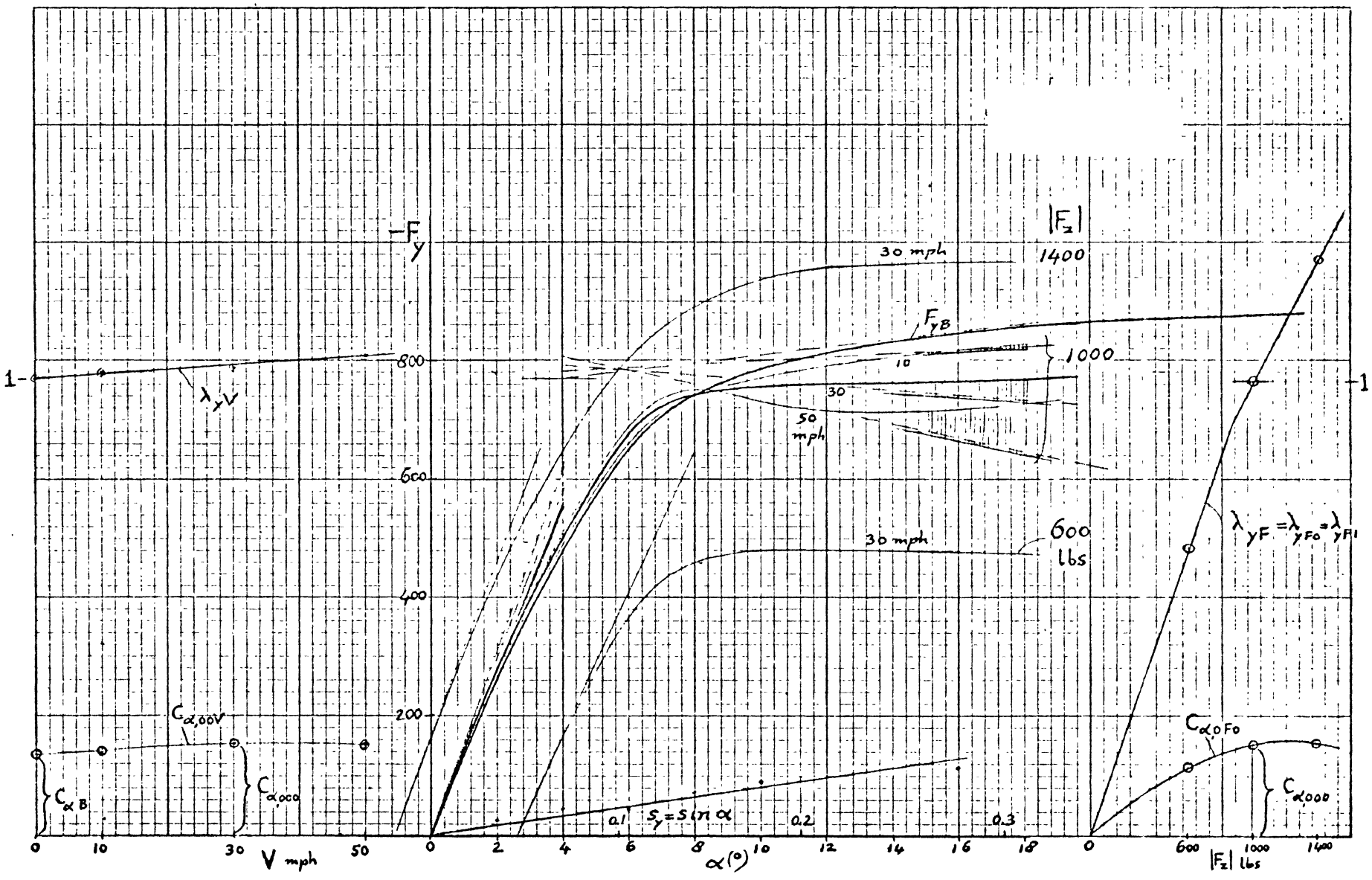

GRAPH I

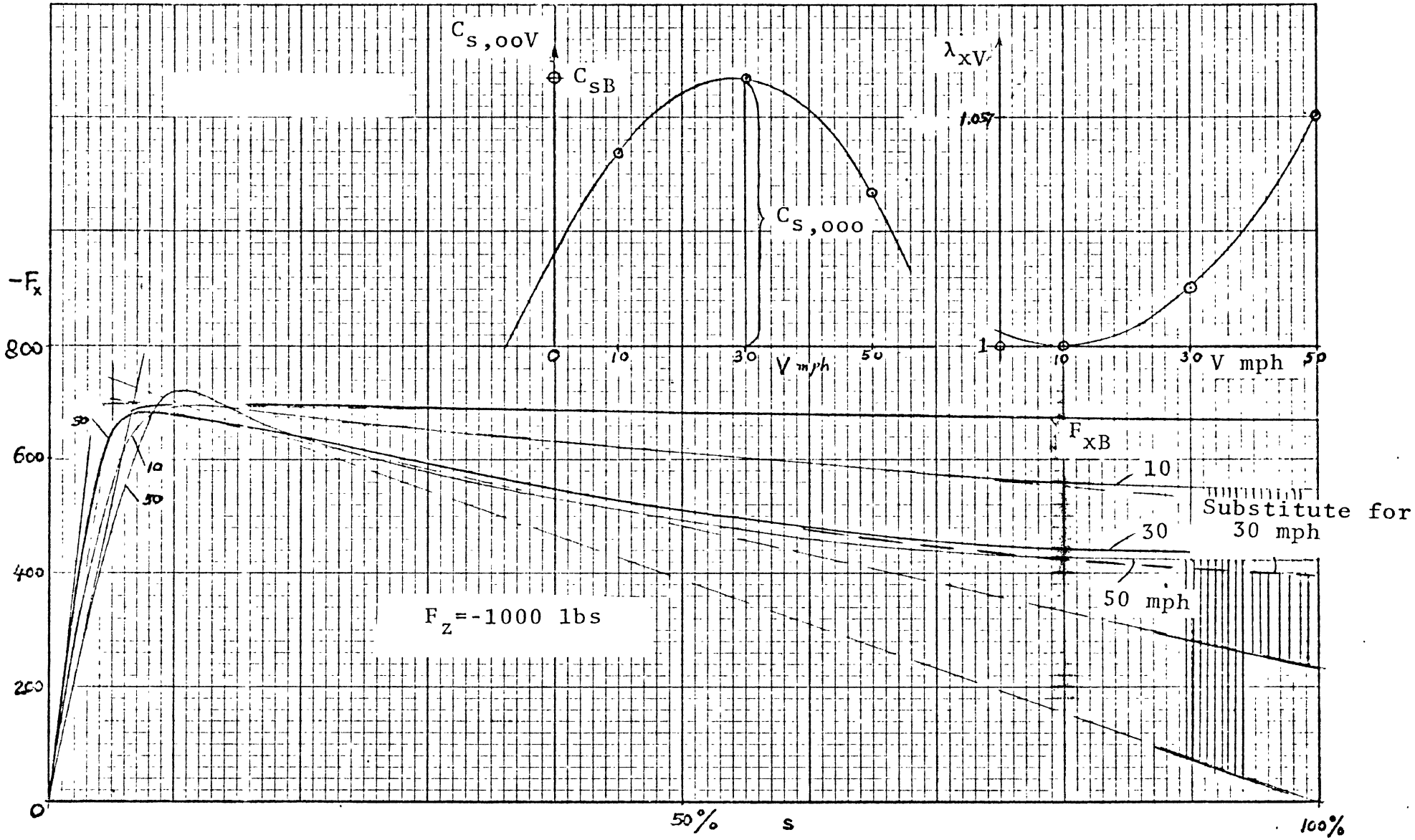
$C_{s,ooV}$
C_{sB}
$C_{s,ooo}$
λ_{xV}
1.057
1
0
10
30
V mph
50
$-F_x$
800
600
400
200
0
F_{xB}
10
30
50 mph
Substitute for 30 mph
F_z=-1000 lbs
50%
s
100%

GRAPH II

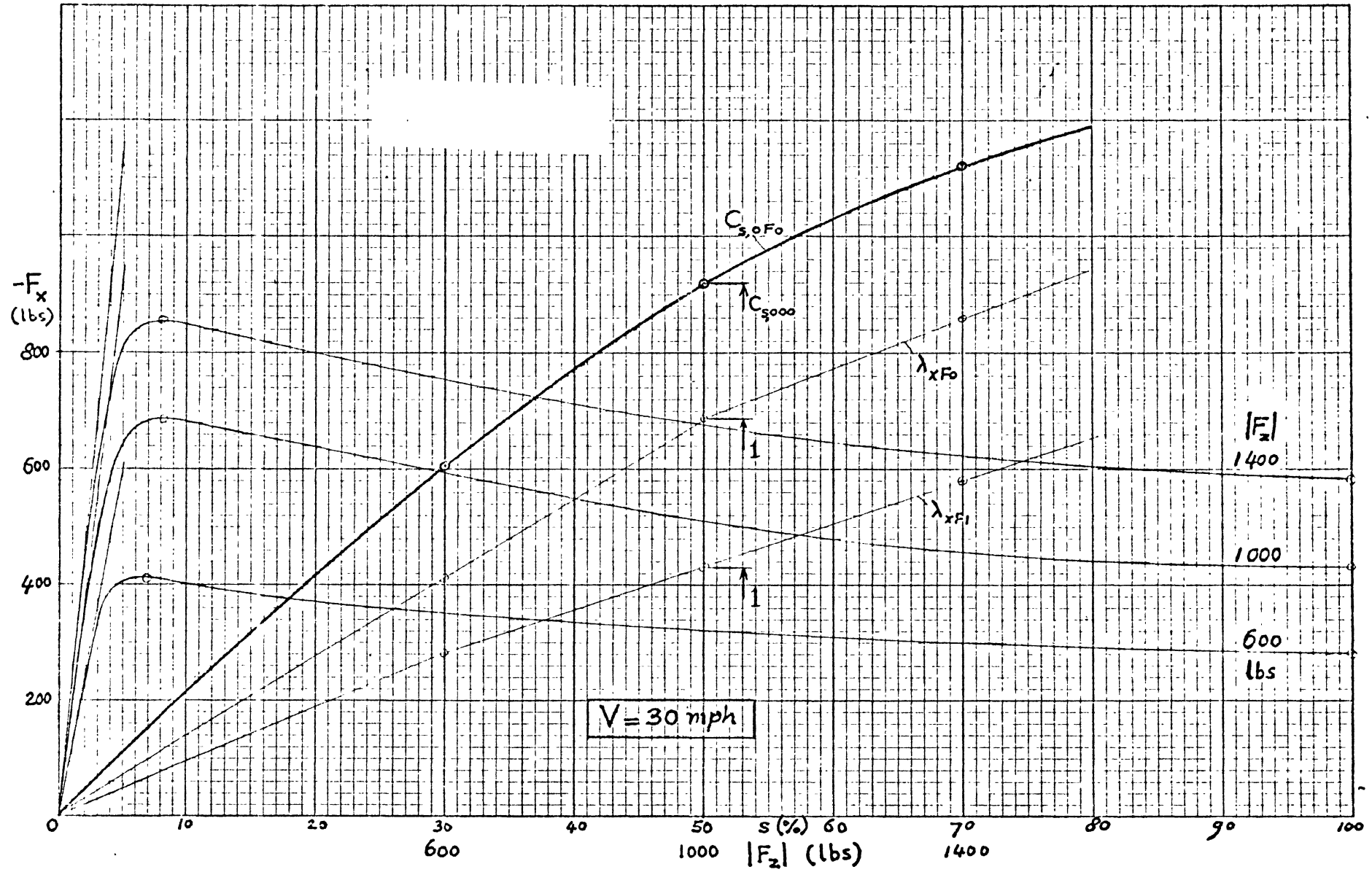
$-F_x$ (lbs)
800
600
400
200
0
10
20
30
40
50
s (%)
60
70
80
90
100
600
1000
$|F_z|$ (lbs)
1400
$C_{s,oFo}$
C_{s000}
λ_{xFo}
λ_{xF1}
1
1
$|F_z|$
1400
1000
600
lbs
V = 30 mph

GRAPH III

NEW RADIAL H-5, ASPHALT

LOAD 1000# , SPEED 30 MPH

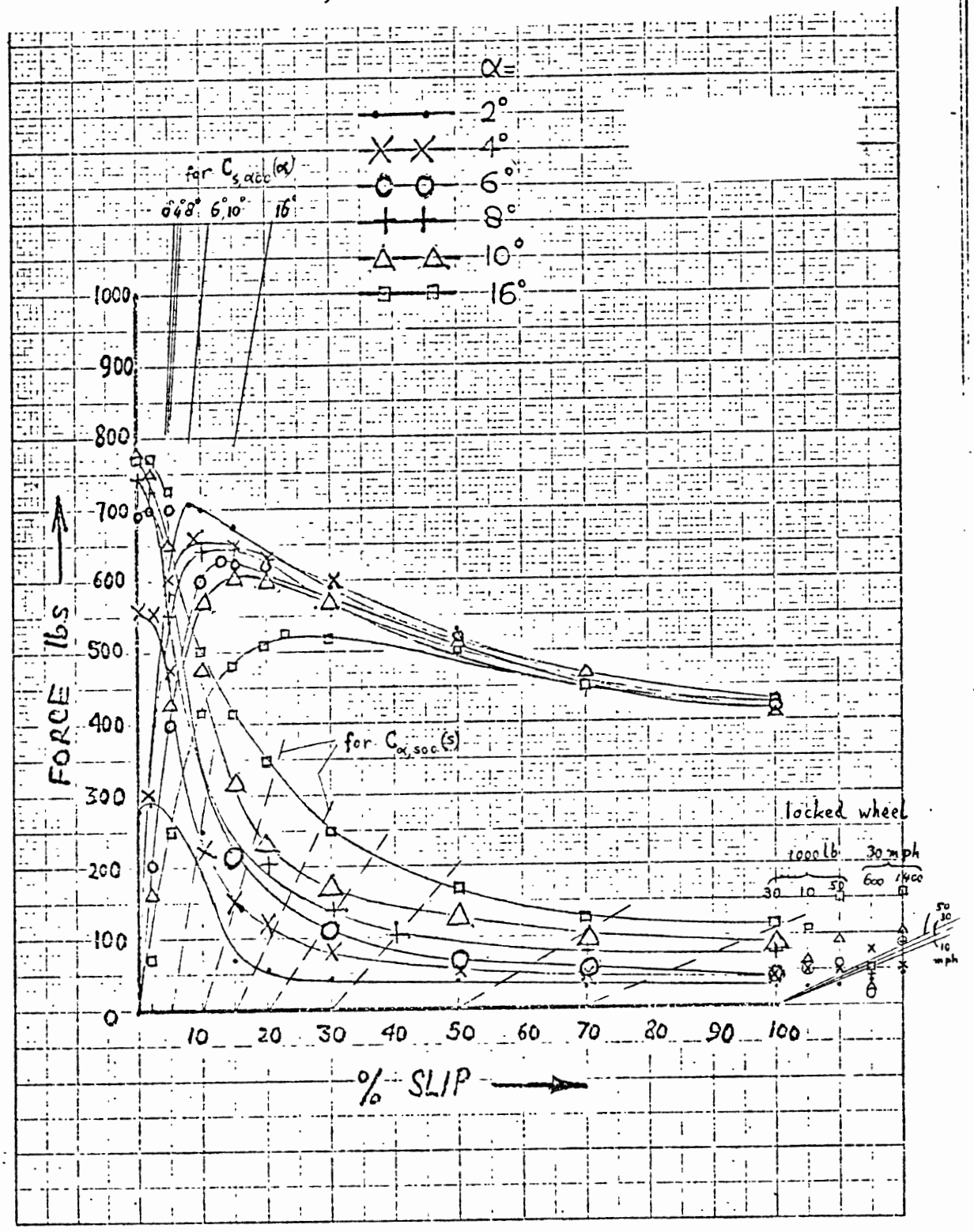

GRAPH IV

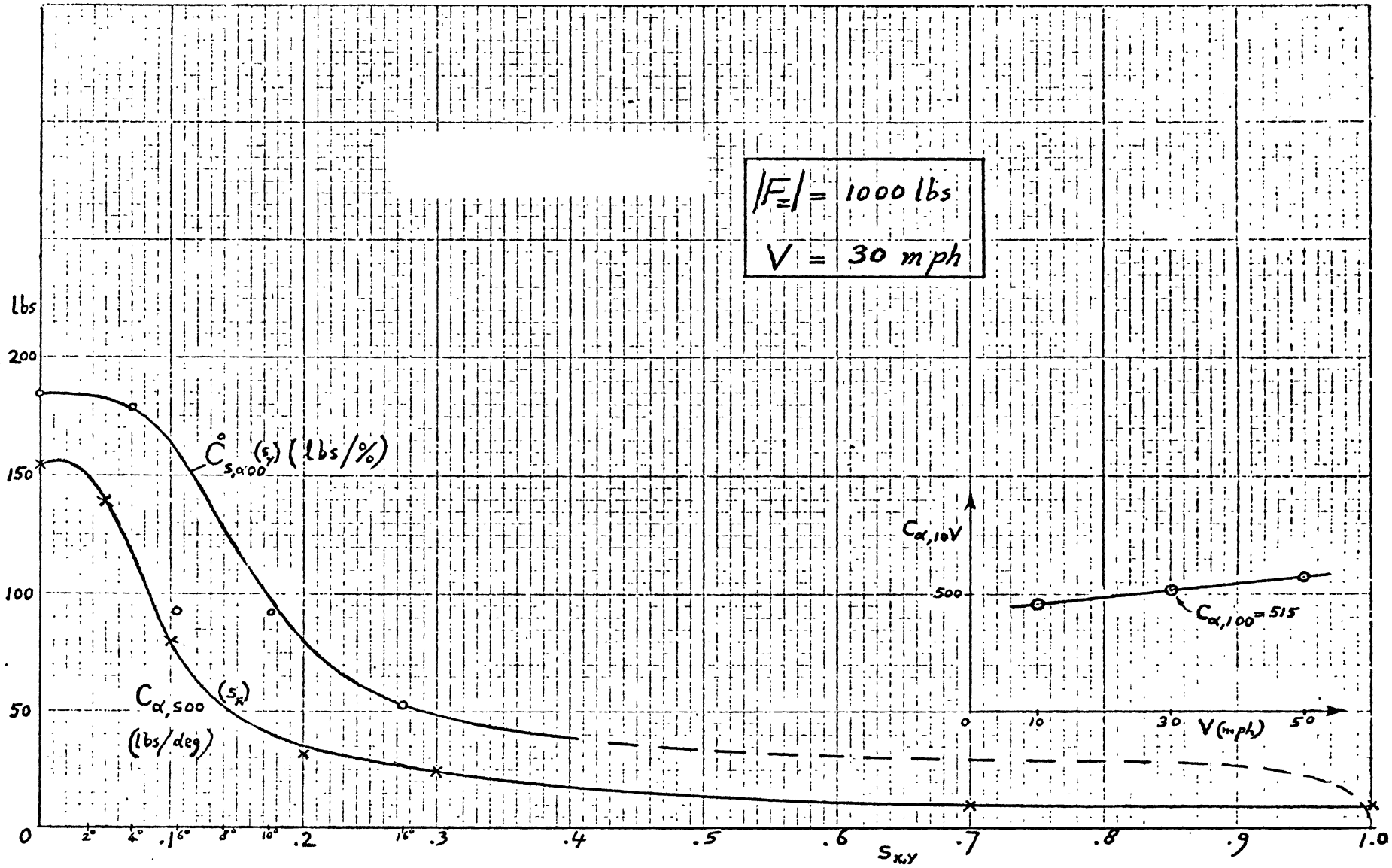
|Fz| = 1000 lbs
V = 30 mph
lbs
200
150
100
50
0
$C^{\circ}_{s,\alpha,00}$ (sy) (lbs/%)
$C_{\alpha,500}$ (sx) (lbs/deg)
$C_{\alpha,10V}$
500
$C_{\alpha,100}$ = 515
0
10
30
V (mph)
50
2°
4°
.1
6°
8°
10°
.2
16°
.3
.4
.5
.6
.7
.8
.9
1.0
$S_{x,y}$

GRAPH V

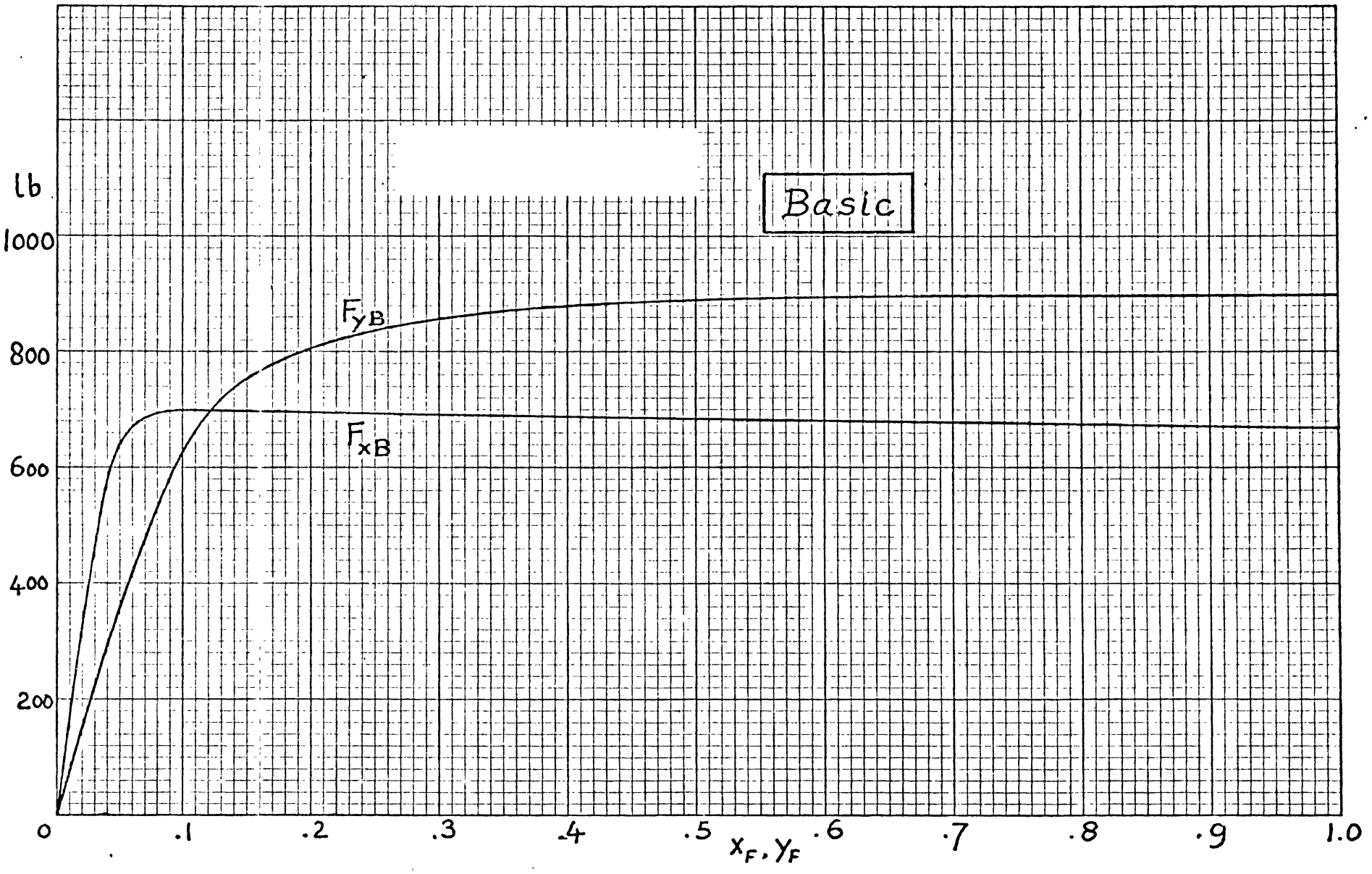

GRAPH VI

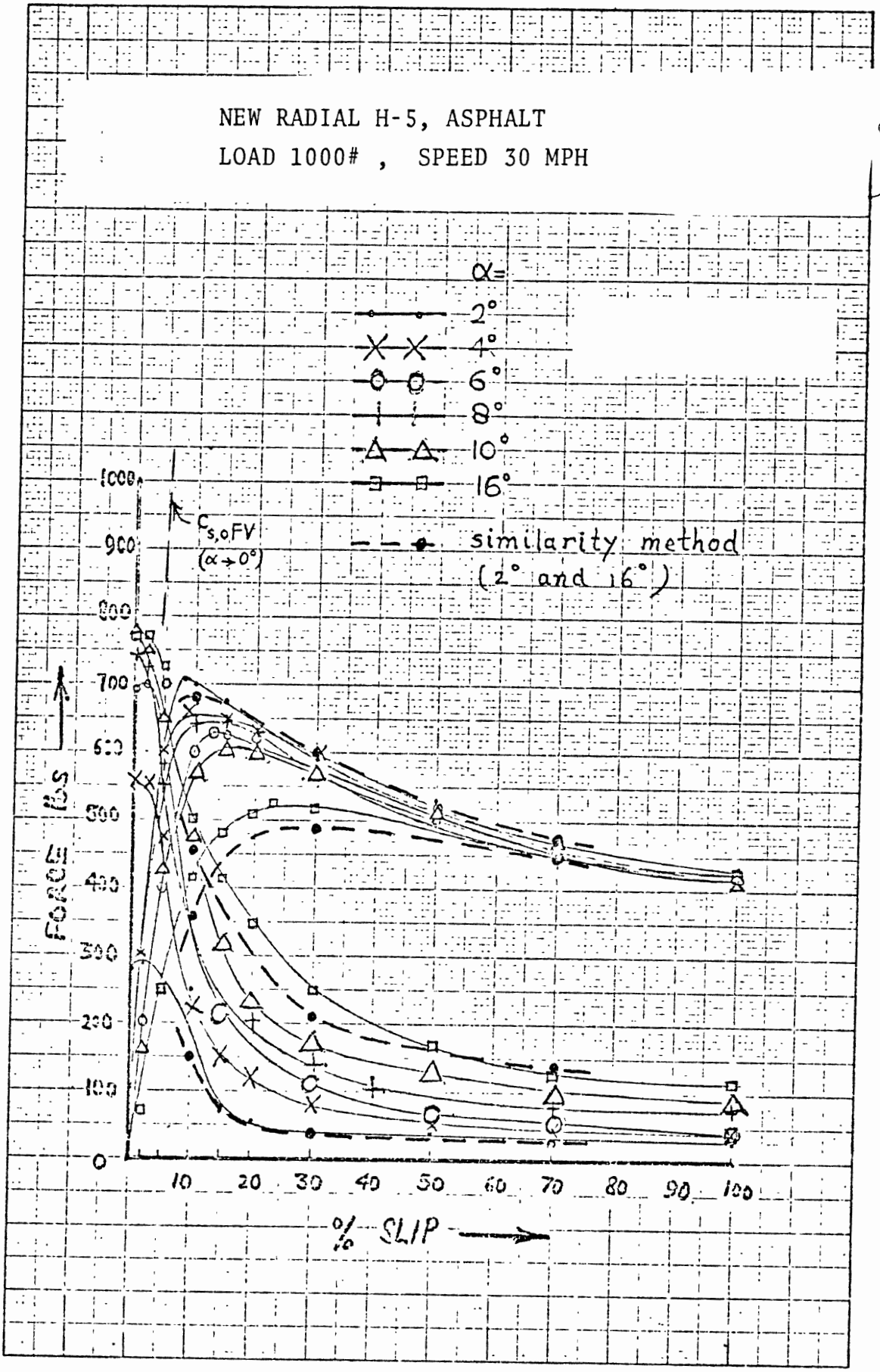
NEW RADIAL H-5, ASPHALT
LOAD 1000# , SPEED 30 MPH
α=
2°
4°
6°
8°
10°
16°
similarity method
(2° and 16°)
$C_{s,o}FV$
(α→0°)
FORCE lbs
1000
900
800
700
600
500
400
300
200
100
0
10
20
30
40
50
60
70
80
90
100
% SLIP

GRAPH VII

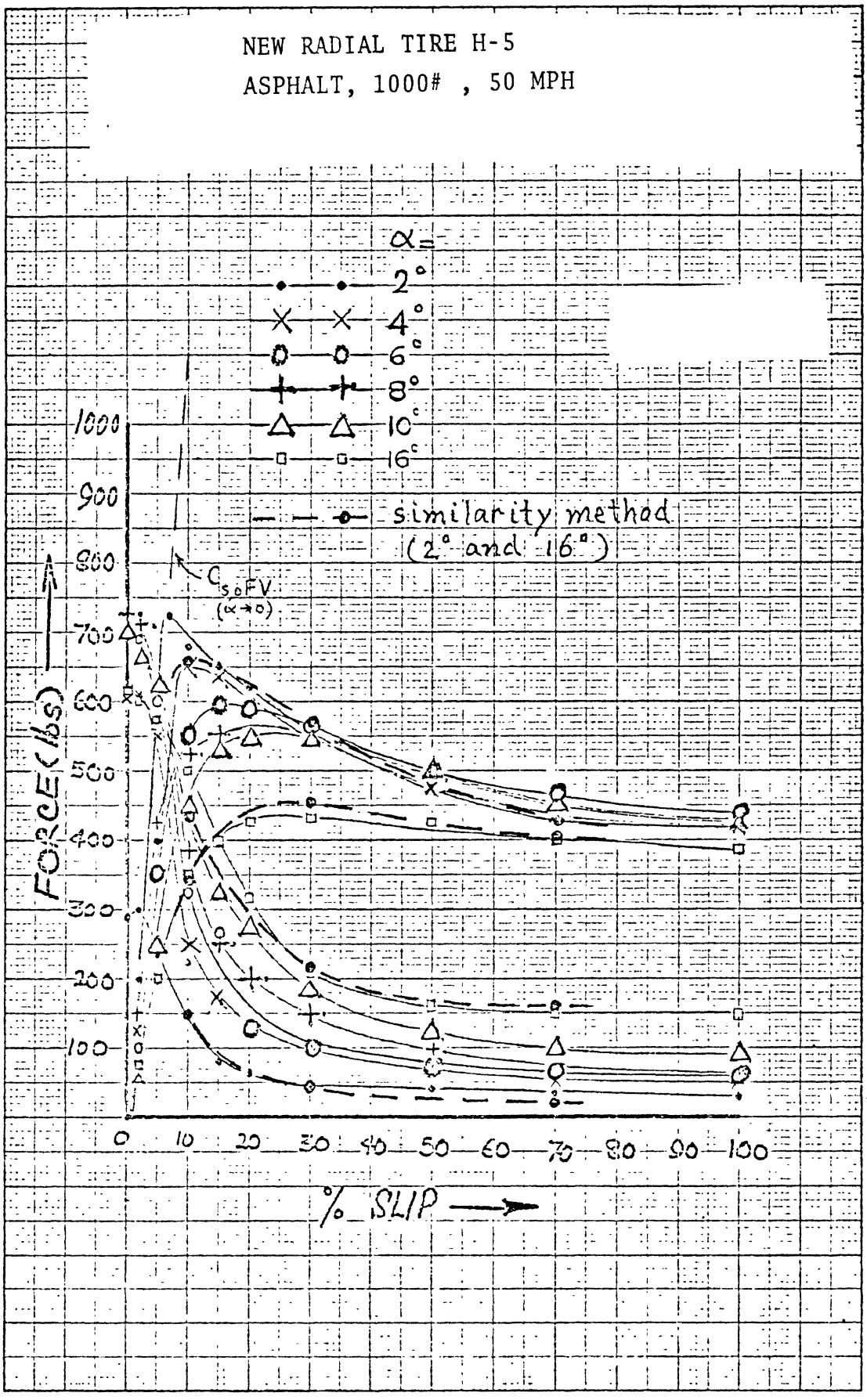
NEW RADIAL TIRE H-5
ASPHALT, 1000# , 50 MPH
α =
2°
4°
6°
8°
10°
16°
similarity method
(2° and 16°)
C_{s_0FV}
(α → 0)
FORCE (lbs)
1000
900
800
700
600
500
400
300
200
100
0
10
20
30
40
50
60
70
80
90
100
% SLIP

GRAPH VIII